

1  
2  
3  
4  
5  
6  
7  
8  
9  
10  
11  
12  
13  
14  
15  
16  
17  
18  
19  
20  
21  
22

**Orbitofrontal cortex neurons code utility changes during natural reward consumption as correlates of relative reward-specific satiety**

**Alexandre Pastor-Bernier, Arkadiusz Stasiak and Wolfram Schultz\***

Department of Physiology, Development and Neuroscience  
University of Cambridge  
Cambridge CB2 3DY  
United Kingdom

**Corresponding Author:** Wolfram Schultz  
Email: [Wolfram.Schultz@protonmail.com](mailto:Wolfram.Schultz@protonmail.com)

**Author Contributions:** APB and WS designed the experiment, APB conducted experiments, APB and AS analyzed data, APB and WS wrote the paper.

**Competing Interests:** The authors declare no competing interests.

**Keywords:** Stochastic choice, psychophysics, indifference curve, revealed preference, multi-component choice option

23

## 24 **Abstract**

25

26 Natural, on-going reward consumption can differentially reduce the subjective value ('utility') of  
27 specific rewards, which indicates relative, reward-specific satiety. Two-dimensional choice  
28 indifference curves (IC) represent the utility of choice options with two distinct reward components  
29 ('bundles') according to Revealed Preference Theory. We estimated two-dimensional ICs from  
30 stochastic choices and found that natural on-going consumption of two bundle rewards induced  
31 specific IC distortions that indicated differential reduction of reward utility indicative of relative  
32 reward-specific satiety. Licking changes confirmed satiety in a mechanism-independent manner.  
33 Neuronal signals in orbitofrontal cortex (OFC) that coded the value of the chosen option followed  
34 closely the consumption-induced IC distortions within recording periods of individual neurons. A  
35 neuronal classifier predicted well the changed utility inferred from the altered behavioral choices.  
36 Neuronal signals for more conventional single-reward choice options showed similar relationships  
37 to utility alterations from on-going consumption. These results demonstrate a neuronal substrate for  
38 the differential, reward-specific alteration of utility by on-going reward consumption reflecting  
39 reward-specific satiety.

40

41

## 42 **Significance**

43

44 Repeated delivery reduces the subjective value ('utility') of rewards to different degrees depending  
45 on their individual properties, a phenomenon commonly referred to as sensory-specific satiety. We  
46 tested monkeys during economic choice of two-component options. On-going consumption  
47 differentially reduced reward utility in a way that suggested relative reward-specific satiety between  
48 the two components. Neurons in the orbitofrontal cortex (OFC) changed their responses in close  
49 correspondence to the differential utility reduction, thus representing a neuronal correlate of relative  
50 reward-specific satiety. Control experiments with conventional single-component choice showed  
51 similar satiety-induced differential response reductions. These results are compatible with the  
52 notion of OFC neurons coding crucial decision variables robustly across different satiety levels.

53

54  
55  
56  
57  
58  
59  
60  
61  
62  
63  
64  
65  
66  
67  
68  
69  
70  
71  
72  
73  
74  
75  
76  
77  
78  
79  
80  
81  
82  
83  
84  
85  
86  
87  
88  
89  
90  
91  
92  
93  
94  
95  
96  
97  
98  
99  
100  
101  
102  
103  
104  
105

## Introduction

Consumption of rewards can reduce their attraction. A classic case is food consumption. While eating a meal of vegetables and meat, we may soon come to prefer the vegetables and stop eating the meat. From these choices, we infer that the vegetables have lost less value for us than the meat. Such consumption-induced specific value loss is often referred to as sensory-specific satiety. Experimentally, sensory-specific satiety is achieved by satiation with one particular reward without altering the intake of another, control reward. Satiation can be induced in several ways. Explicit tests consist of rapidly and abundantly feeding with a test reward. Its controlled nature makes this method popular for studying the effects of general or sensory-specific satiety on neuronal and behavioral functions of orbitofrontal cortex (OFC) and midbrain (Rolls et al., 1989; Critchley and Rolls, 1996; Small et al., 2001; Kringelbach et al., 2003; Gottfried et al., 2003; Izquierdo et al. 2004; Bouret & Richmond, 2010; Rudebeck et al., 2013; Murray et al., 2015). Another explicit but less artificial test consists of repeatedly feeding smaller quantities while conducting intervening tests (Yaxley et al., 1985; Rolls et al. 1988). Opposite to intentional induction, spontaneous variations in thirst and hunger change the subjective reward value while keeping physical properties unchanged and serve for identifying subjective reward value signals in monkey OFC (Padoa-Schioppa & Assad, 2006). Despite the multitude of these heterogeneous data, satiety tests that combine controllability with natural satiation are scarce. Such tests should involve neither bolus administration nor spontaneous thirst or hunger variations.

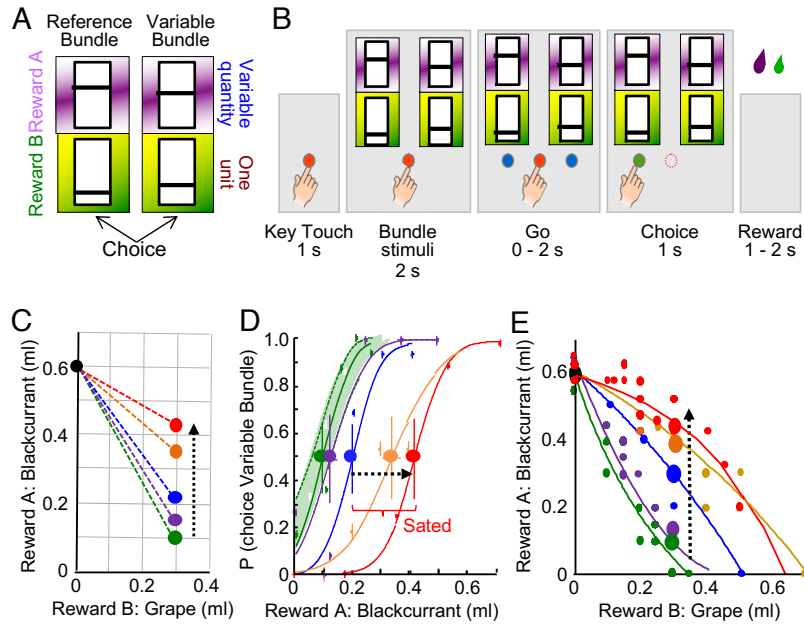
Testing reward-specific satiety requires comparison between a reward on which an animal is sated and another reward on which the animal is less or not sated. This two-reward requirement matches the fact that choice options can have multiple components. For example, a meal is composed of vegetables and meat, and choosing a particular meal concerns both food stuffs. The multi-component nature is conceptualized in Revealed Preference Theory; its two-dimensional indifference curves (IC) graphically display reward preferences that are revealed by measurable choice (Fisher, 1892; Samuelson, 1937; Samuelson, 1938). The preferences may be fixed, as the theory assumes, or they may be constructed on the fly at the time of choice (Payne, Bettman, & Schkade, 1999; Simonson, 2008; Dhar & Novemsky, 2008; Kivetz, Netzer & Schrift, 2008; Warren, McGraw & Van Boven, 2011). We estimated ICs in rhesus monkeys that represented their revealed preferences for multi-component reward bundles in an orderly manner. The animals' choices satisfied necessary requirements for rationality, including completeness (preference for one or the other option, or indifference), transitivity, and independence of option set size (Pastor-Bernier et al., 2017). These tests with two-component choice options seem appropriate for testing reward-specific satiety with two differentially sated rewards. Specifically, as ICs represent the integrated economic utility of all bundle rewards, how would a change in the utility of one bundle reward relative to the other reward change the IC shape? And how would neuronal responses reflect these relative utility changes? During typical experimental sessions, the natural on-going consumption of the two bundle rewards would allow to study differential utility changes reflecting relative reward-specific satiety, without requiring artificial bolus administration or spontaneous variations in thirst or hunger.

Here we used the IC scheme to investigate the influence of natural, on-going reward consumption on OFC neurons. We built on our earlier study on OFC neurons whose responses followed the IC scheme; monotonic change with increasing utility irrespective of specific bundle composition, and equal response with equally preferred but differently composed bundles (Pastor-Bernier et al., 2019). We now report that neuronal reward signals in OFC followed the systematically changed ICs that reflected differential reward value changes from natural, on-going reward consumption during the recording period of individual neurons, compatible with the notion of relative, reward-specific satiety. In doing so, OFC neurons coded the integrated economic utility of all bundle rewards in a systematic and conceptually defined manner.

106 **Results**

107

108 We presented the monkey simultaneously with two composite stimuli on a horizontally mounted  
 109 touch screen (binary choice task with two discrete, mutually exclusive and collectively exhaustive  
 110 options; Figure 1A, B). Two rectangles in each stimulus represented a bundle with two reward  
 111 components whose individual amounts were indicated by a vertical bar (higher was more). The two  
 112 components were blackcurrant juice or blackcurrant juice with added monosodium glutamate  
 113 (MSG) in all bundle types as Reward A, and grape juice, strawberry juice, mango juice, water,  
 114 apple juice, peach juice or grape juice with added inosine monophosphate (IMG) as Reward B.  
 115

116  
117118 **Figure 1. Task, design and behavior**

119 (A) Choice options. Each bundle contained two rewards (A, B) with independently set amounts indicated by  
 120 the vertical bar position within each rectangle (higher was more). The Reference Bundle contained two  
 121 preset reward amounts. The Variable Bundle contained a specific amount of one reward and an  
 122 experimentally varied amount of the other reward.

123 (B) Task sequence: In each trial the animal contacted a central touch key for 1.0 s; then the two choice  
 124 options appeared on a computer monitor. After 2.0 s, two blue spots appeared on the monitor, and the  
 125 animal touched one option within 2.0 s. After touching the target for 1.0 s, the blue spot underneath the  
 126 chosen bundle turned green as feedback for successful selection, and the blue spot disappeared. The  
 127 computer-controlled liquid solenoid valve delivered Reward A at 1.0 s after the choice, and Reward B 0.5 s  
 128 later.

129 (C) Simplified test scheme: relative reward-specific satiety indicated by decreasing trade-off. With on-going  
 130 consumption of both juices, the animal gave up progressively less blackcurrant juice for obtaining the same  
 131 amount (0.3 ml) of grape juice while maintaining choice indifference between the black and one of the  
 132 colored bundles (from green to red), suggesting utility loss of grape juice relative to blackcurrant juice.

133 (D) Psychophysical assessment of choice between constant Reference Bundle (0.6 ml blackcurrant juice, 0.0  
 134 ml grape juice) and Variable bundle (varying reward A, blackcurrant juice, from 0 to 0.7 ml, while holding  
 135 grape juice constant at 0.3 ml) (same bundles as in C). Green and violet curves inside green  $\pm 95\%$   
 136 confidence intervals (CI): initial choices; blue, orange and red curves: on-going consumption; heavy dots:  
 137 indifference points (IP). Satiety was defined by IPs exceeding CIs. Each curve and IP were estimated from  
 138 80 trials in a single block (Weibull fits, Monkey A).

139 (E) Gradual changes in slope and curvature of ICs between pre-satiety (green, violet) and during increasing  
 140 satiety (blue, orange, red). Each IC was estimated from fitting to about 35 IPs (Eq. 1), with 80 trials/IP  
 141 (Monkey A). Small dots indicate IPs, large dots indicate IPs estimated from a single psychophysical test  
 142 sequence (as shown in (D) with same color convention but from different session).  
 143

## 144 **Basic behavioral design**

145 Our study followed the notions that subjective reward value (utility) can be inferred from  
 146 observable economic choice, that altered choice would indicate a change in utility, and that a  
 147 reduction of utility from natural, on-going consumption reflects satiety. The assessment of  
 148 differential, reward-specific utility change requires at least two rewards. We tested choices between  
 149 bundles that each had two liquid rewards whose independently variable amounts were represented  
 150 at the axes and interior of two-dimensional graphs (Figure 1C). We investigated neuronal activity in  
 151 repeated trials for reasons of statistics and thus tested stochastic, rather than single-shot, choices that  
 152 are often used on humans.

153 Pilot tests of all rewards had indicated that blackcurrant juice was least prone to satiety,  
 154 possibly reflecting taste and/or sugar content differences. Therefore, we designated blackcurrant  
 155 juice as Reward A for the y-axis of the two-dimensional graph, whereas all other liquids constituted  
 156 Reward B and were plotted on the x-axis. This convention allowed us to estimate the relative value  
 157 of all rewards in the common currency of blackcurrant juice at choice indifference.

158 In choice between two bundles, relative reward utility is inferred from the amount of the  
 159 bundle reward the animal gives up in order to gain one unit of the other reward of the same bundle,  
 160 without change in bundle utility (Marginal Rate of Substitution, MRS); unchanged bundle utility is  
 161 evidenced by maintained equal preference in the trade-off between the old bundle and the new  
 162 bundle (choice probability of  $P = 0.5$  for each option) (Figure 1C, black dot vs. colored dots). By  
 163 contrast, a binary choice between a single reward and its alternative does not amount to a trade-off  
 164 in the stricter sense of giving up something one already has for obtaining something one does not  
 165 yet have; in this more simple binary choice, either one or the other reward is obtained but nothing  
 166 already owned is given up. With the true trade-off during multi-component bundle choice, only  
 167 parts of each bundle are exchanged, and any relative utility change with on-going reward  
 168 consumption is manifested as altered trade-off slope between the two bundles being chosen (black  
 169 dot vs. colored dots; MRS change). In addition to allowing a true trade-off, the design with two  
 170 bundle components allows to test bundles with intermediate values between the x- and y-axes.

171

## 172 **Consumption-induced relative utility reduction**

173 At the onset of a daily experiment, the black and green bundles of Figure 1C were chosen with  
 174 equal probability. When choosing the green bundle, the animal gave up 0.5 ml of blackcurrant juice  
 175 (from 0.6 ml to 0.1 ml) to gain 0.3 ml of grape juice. With on-going consumption of both juices the  
 176 value ratio between the rewards (trade-off amount) changed: to gain the same 0.3 ml amount of  
 177 grape juice, the animal gave up progressively less blackcurrant juice, from 0.45 ml via 0.38 ml and  
 178 0.25 ml to finally only 1.8 ml (Figure 1C; upward arrow, from violet via blue and orange to red).  
 179 Thus, the slope between the two bundles on the two-dimensional graph changed as the animal  
 180 'payed' progressively less blackcurrant juice for the same amount of grape juice.

181 We set both rewards in the Reference Bundle, and one reward of the Variable Bundle, to  
 182 specific amounts, varied psychophysically the amount of the other Variable Bundle reward over the  
 183 whole testing range, and then fitted a Weibull function to the choice probabilities in order to  
 184 estimate the amount of the variable reward at which both bundles were chosen with equal  
 185 probability. For example, in choices between a Reference Bundle, which contained only  
 186 blackcurrant juice, and a Variable Bundle with fixed amount of grape juice and variable amount of  
 187 blackcurrant juice, on-going consumption of both juices required increasing amounts of  
 188 blackcurrant juice for choice indifference (Figure 1D, heavy dots). The rightward shift of the  
 189 indifference point (IP) from green via violet, blue and orange to red indicated that the animal  
 190 became gradually more reluctant to give up blackcurrant juice for obtaining the same amount of  
 191 grape juice; apparently, grape juice had lost more value compared to blackcurrant juice. As each IP  
 192 was estimated psychophysically in 80 trials, satiety as studied here progressed in test blocks rather  
 193 than on a trial-by-trial basis. The initial two IPs were close together (green and violet within green  
 194 95% confidence interval, CI), suggesting initially maintained reward value, whereas the next IPs  
 195 outside the CI were considerably higher and indicated substantial value loss (blue, yellow and red

196 IPs). In other words, the MRS declined with on-going consumption, as schematized in Figure 1C.  
 197 We assumed that the value change inferred from IP positions outside the CI indicated satiety.

198 At choice indifference between the two bundles, the amounts of the two Variable Bundle  
 199 rewards defined an IP (Figure 1E). A new IP was obtained by setting the Reference Bundle to a  
 200 previously estimated IP position, then setting one reward of the Variable Bundle to a specific  
 201 amount, varying its other reward psychophysically and estimating choice indifference from curve  
 202 fitting. Repetition of this procedure, in pseudorandomly alternating directions to avoid local  
 203 distortions (Knetsch, 1989), resulted in a series of equally preferred IPs. We used these IPs to fit  
 204 two-dimensional indifference curves (IC) whose slope and curvature reflected the utility of one  
 205 bundle reward relative to the other bundle reward (Figure 1E; see Methods; Eq. 1). Thus, on-going  
 206 reward consumption resulted not only in slope change (Figure 1C) but in more informative  
 207 monotonic IC curvature change from convex (green) via near-linear (blue) to concave (red), which  
 208 provided systematic evidence for the animal's increasing reluctance to give up blackcurrant juice  
 209 unless receiving more substantial amounts of grape juice. Both IC changes characterized in a  
 210 systematic manner the differential reduction of utility of grape juice relative to blackcurrant juice  
 211 during on-going consumption of both juices, which suggested relative reward-specific satiety for  
 212 grape juice. These two-dimensional changes were measured during recording periods of individual  
 213 neurons and constituted our test scheme for behavioral and neuronal correlates of satiety.

214 For more simple numeric value assessment, we positioned single-component bundles on the  
 215 x-and y-axes and studied only the ratio between equally preferred rewards, which was graphically  
 216 represented as two-dimensional slope change (anchor trials). We held blackcurrant juice constant  
 217 and psychophysically varied grape juice to obtain an IP (Figure S1A-C). With on-going reward  
 218 consumption, the animal gave up the same constant blackcurrant juice amount only when gaining  
 219 monotonically increasing grape juice amounts at IP. This change reduced the ratio  
 220 blackcurrant:grape juice required for choice indifference and suggested relative value reduction of  
 221 grape juice. The IC curvature showed similar flattening and frequent transition from convex to  
 222 concave as with the original testing scheme (Figure S1D). The ICs with Monkey B showed similar  
 223 slope flattening (Figure S1E, F). These tests demonstrate robust value reduction of grape juice with  
 224 on-going consumption irrespective of the test scheme employed.

### 225 226 **Consistency across different bundles**

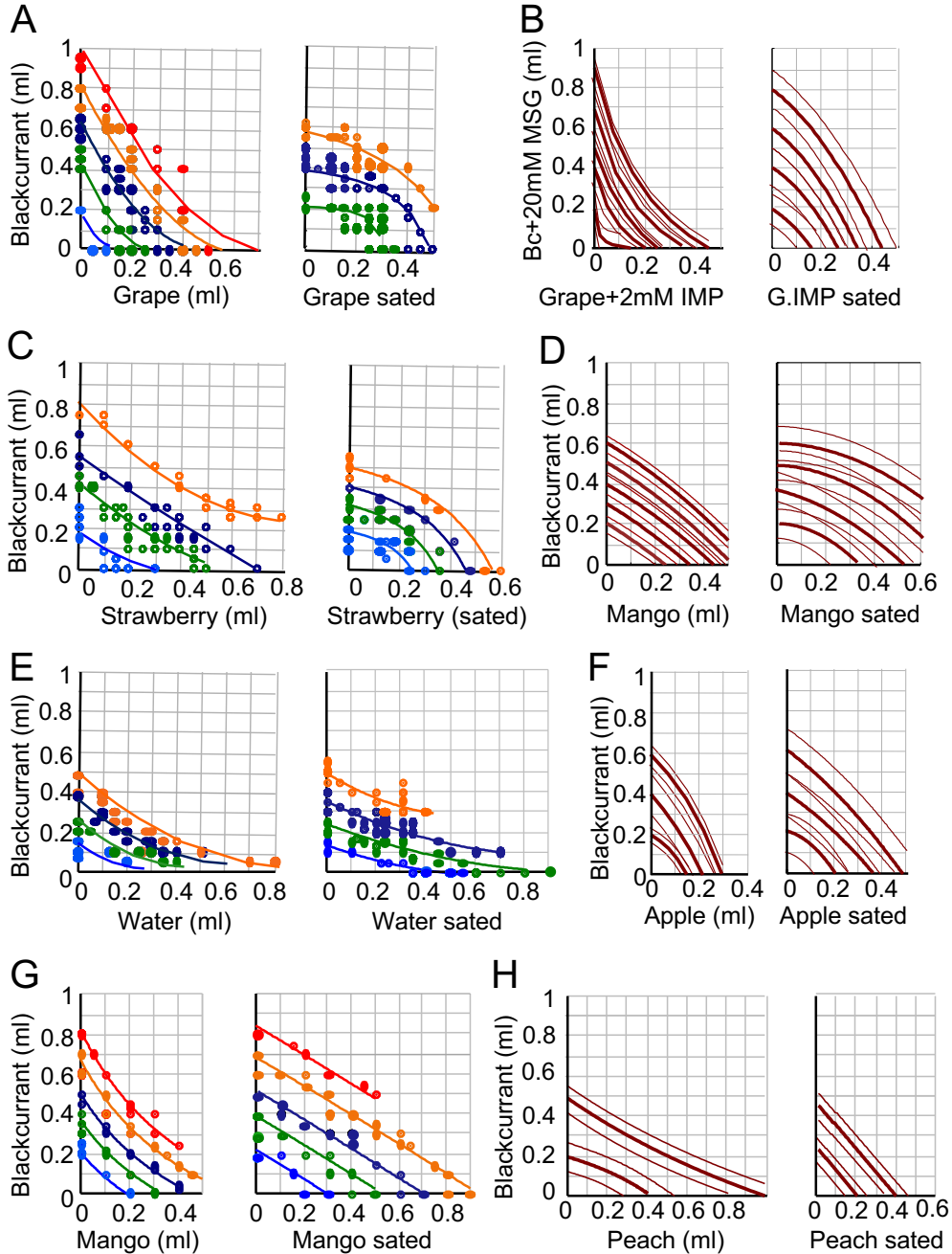
227 Two rhesus monkeys performed 74,659 trials with the eight bundle types (Figure 2). Given that  
 228 relative reward-specific satiety would change the ratio of reward amounts at IPs, and the  
 229 observation that animals sated least on blackcurrant juice, we defined the boundary between pre-  
 230 sated and sated states by the CI of the initial, left-most choice function between blackcurrant juice  
 231 and any reward (green in Figures 1D, S1A and S1E); any IP outside this interval indicated utility  
 232 reduction.

233 Before satiety, we used a total of 38,443 trials to estimate 56 IPs for fitting 5 ICs with the  
 234 bundle (blackcurrant juice, grape juice), 68 IPs for 4 ICs with bundle (blackcurrant juice, strawberry  
 235 juice), 58 IPs for 4 ICs with bundle (blackcurrant juice, water), 38 IPs for 5 ICs with bundle  
 236 (blackcurrant juice, mango juice) (Monkey B), 65 IPs for 5 ICs with bundle (blackcurrant+MSG,  
 237 grape+IMP), 55 IPs for 5 ICs with bundle (blackcurrant juice, mango juice), 45 IPs for 3 ICs with  
 238 bundle (blackcurrant juice, apple juice), and 40 IPs for 2 ICs with bundle (blackcurrant juice, peach  
 239 juice) (Monkey B).

240 During satiety, we used 36,216 trials to estimate 52 IPs for 3 ICs with bundle (blackcurrant  
 241 juice, grape juice), 37 IPs for 4 ICs with bundle (blackcurrant juice, strawberry juice), 63 IPs for 4  
 242 ICs with bundle (blackcurrant juice, water), 48 IPs for 5 ICs with bundle (blackcurrant juice, mango  
 243 juice) (Monkey B), 49 IPs for 4 ICs with bundle (blackcurrant+MSG, grape+IMP), 52 IPs for 4 ICs  
 244 with bundle (blackcurrant juice, mango juice), 55 IPs for 3 ICs with bundle (blackcurrant juice,  
 245 apple juice), and 44 IPs for 2 ICs with bundle (blackcurrant juice, peach juice) (Monkey B).

246 On-going reward consumption induced IC shape changes with all eight bundles in both  
 247 animals (Figure 2). Stronger satiety for 6 of the 8 liquids (x-axis) relative to blackcurrant (y-axis)

248 resulted in flattening of IC slopes and transition from convex to linear and concave curvature  
 249 (Figure S1G, H). However, monkey B seemed to become less satiated on peach juice compared to  
 250 blackcurrant juice, as suggested by steeper ICs (Figure 2H). Together, these IC changes  
 251 demonstrated robust relative utility loss with natural, on-going liquid consumption across a variety  
 252 of bundle types.  
 253



254  
 255

256 **Figure 2. indifference curves reflect relative reward-specific satiety for different bundle types**  
 257 (A) - (F) Behavioral indifference curves (ICs) for all bundle types used in the current experiment with  
 258 Monkey A. Lines show ICs fitted hyperbolicly to indifference points (IP) of same color (Eq. 1). Dots in A,  
 259 C, E show measured IPs (choice indifference between all bundles of same color). Dotted lines in B, D, F  
 260 show  $\pm 95\%$  confidence intervals. Reward A is plotted on the y-axis, Reward B on the x-axis. Bc,  
 261 blackcurrant juice; MSG, monosodium glutamate; IMP, inosine monophosphate. Same color convention in  
 262 (A), (C), (E) and (G) as in Figure 1C, D, E.  
 263 (G), (H) as (A) but for Monkey B.  
 264

265 **Control for other choice variables**

266 A logistic regression served to confirm that bundle choice varied only with the bundle rewards  
 267 rather than unrelated variables with on-going consumption (Eq. 2). As before satiety (Pastor-Bernier  
 268 et al. 2019), the probability of choosing the Variable Bundle continued to correlate positively with  
 269 the amounts of both of its rewards, and inversely with the amounts of both Reference Bundle  
 270 rewards (Figure S1I; VA, VB vs. RA, RB). Further, choice probability for the Variable Bundle was  
 271 anticorrelated with the accumulated consumption of blackcurrant juice (MA) and positively  
 272 correlated with grape juice consumption (MB). This asymmetry is explained by the trade-off at IPs;  
 273 as grape juice lost more utility than blackcurrant juice during satiety, the animal consumed more  
 274 grape juice and gave up less blackcurrant juice. Trial number within individual trial blocks (CT) and  
 275 spatial choice CL) did not explain the choice. Thus, even with on-going consumption, the animals  
 276 based their choice on the reward amounts of the bundles and the actually consumed rewards  
 277 according to the experimental design; unrelated variables kept having no significant influence.

278

279 **Licking and liquid consumption**

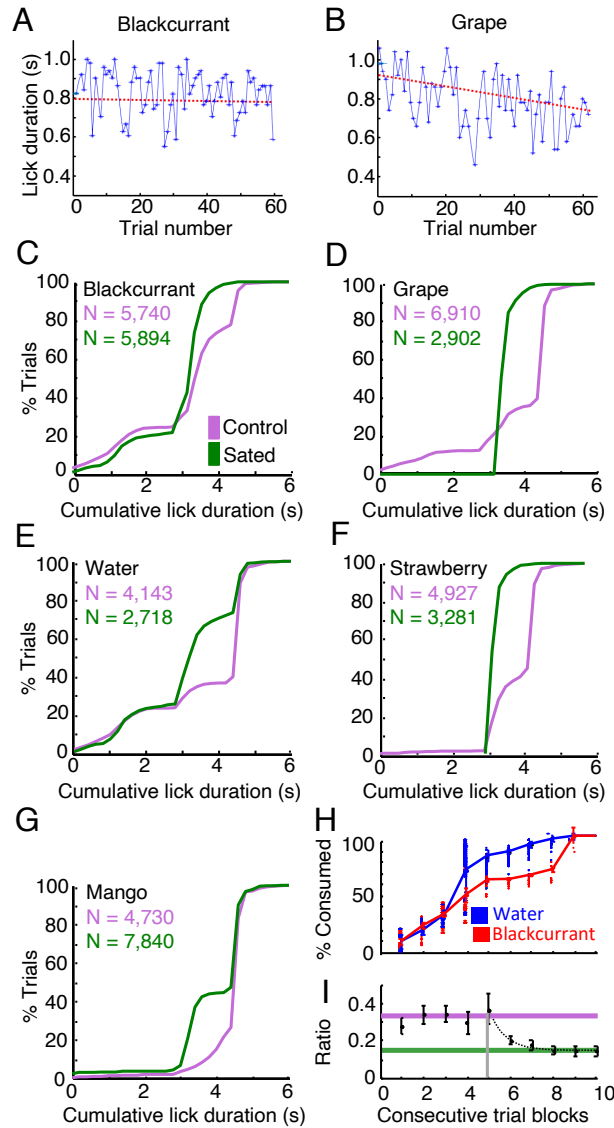
280 Lick durations are crude measures for subjective reward value but could serve as mechanism-  
 281 independent confirmation for the utility changes seen with the choices. Trial-by-trial time courses of  
 282 lick durations with on-going consumption showed gradual and asymmetric decreases for the bundle  
 283 rewards (Figure 3A, B). Lick durations remained nearly constant for blackcurrant juice (slope = -  
 284 2.86 deg,  $R^2 = 0.56$ ; linear regression) but decreased strongly for grape juice (slope = -20.6 deg,  $R^2$   
 285 = 0.50), suggesting stronger utility loss for grape juice compared to blackcurrant juice. Cumulative  
 286 licking was significantly shorter in the sated state (green) compared to the pre-sated state (pink)  
 287 with the main liquids tested in both monkeys (Figure 3C-G). Thus, the reward value changes  
 288 inferred from lick durations corresponded in direction to those inferred from IC slope and curvature  
 289 changes (Figure 2).

290 The IC flattening with on-going consumption indicated that the animal required increasing  
 291 amounts of the more devalued Reward B for giving up the same amount of the less devalued  
 292 blackcurrant juice (Reward A) at trade-off. This change was particularly evident in choice between  
 293 the constant Reference Bundle containing only blackcurrant juice (Reward A) and the Variable  
 294 Bundle containing only one of the other liquids (Reward B) (Figure S1A, B; increase on x-axis).  
 295 With on-going consumption, the animal gave up the same amount of the less sated blackcurrant  
 296 juice only if it received increasingly more of the sated Reward B at choice indifference. As the  
 297 animal had no control over the constant Reference Bundle that defined the IP, the animal ended up  
 298 consuming more of the devalued reward as the session advanced. For example, with the bundle  
 299 (blackcurrant juice, water), water consumption increased with beginning satiety more than that of  
 300 blackcurrant juice (Figure 3H; blue vs. red;  $P = 5.0979 \times 10^{-7}$ ; Kolmogorov-Smirnov test;  $N = 7,160$   
 301 trials), thus decreasing the ratio of consumed blackcurrant:water amounts at IP (Figure 3I).

302 Consumption in bundles containing blackcurrant juice together with grape juice, water, strawberry  
 303 juice or mango juice correlated significantly with their consumption ratios ( $Rho = 0.3859$ ;  $P =$   
 304  $0.0056$ ; Pearson). At the end of daily sessions, animals lost complete interest in water and mostly  
 305 chose the Reference Bundle containing blackcurrant juice alone (right in Figure 3H, not included in  
 306 Figure 3I).

307 Thus, the licking changes confirmed in a mechanism-independent manner the relative reward-  
 308 specific utility changes inferred from bundle choices.

309



310  
311

312 **Figure 3. Anticipatory licking and differential juice consumption**

313 (A), (B) Anticipatory licking with bundles (blackcurrant juice, grape juice) with advancing reward  
314 consumption within single test sessions ( $N = 69$  and  $65$  trials, respectively; Monkey A). Red lines show linear  
315 regressions of lick duration across trials. Lick durations remained nearly constant for blackcurrant juice,  
316 but decreased for grape juice, indicating relative utility loss for grape juice.

317 (C) - (G) Cumulative distributions of lick durations between bundle appearance and reward delivery for  
318 several bundles. Both animals showed significantly more trials with longer lick durations before (pink) than  
319 during satiety (green). Monkey A, blackcurrant juice:  $P = 5.46 \times 10^{-4}$ ; Kolmogorov-Smirnov test;  $N = 5,740 /$   
320  $5,894$  pre-sated/sated trials) grape juice:  $P = 2.59 \times 10^{-9}$ ;  $N = 6,910 / 2,902$ , water:  $P = 3.60 \times 10^{-3}$ ;  $N =$   
321  $4,143 / 2,718$ , strawberry juice:  $P = 8.66 \times 10^{-6}$ ;  $N = 4,920 / 3,281$ ; Monkey B, mango juice:  $P = 2.41 \times 10^{-9}$ ;  
322  $N = 4,730 / 7,840$ .

323 (H) Cumulative consumption of water and blackcurrant juice during 10 advancing blocks and 7,160 anchor  
324 trials (each bundle contained only one liquid; see Figure S1A, B for test scheme). For constant blackcurrant  
325 amounts (red), the animal consumed significantly more water than blackcurrant as the session advanced  
326 (Monkey A).

327 (I) Exponential reduction of blackcurrant:water ratio from 0.32 (1:3) to 0.15 (1:6) after initial trials  
328 (vertical grey line). Single exponential function  $f(\beta, x) = \beta_1 + \beta_2 e^{(\beta_3 x)}$ ;  $[\beta_1, \beta_2, \beta_3] = [0.15, 254.78, -1.41]$  ( $\beta_1$ :  
329 final ratio, green line;  $\beta_2$ : decay constant). Consecutive 10 trial blocks for fitting included last block with  
330 stable ratio ( $N = 5,520$  trials; Monkey A).

331

### 332 **Neuronal test design**

333 We used the IC changes with on-going reward consumption observed in a large variety of bundles  
 334 to investigate altered value coding in OFC reward neurons. Given the shallower slopes and the less  
 335 convex and more concave curvatures, we placed bundles on specific segments of the ICs that would  
 336 change with on-going consumption, such that the physically unaltered bundles would end up on  
 337 different ICs or IC parts. We subjected most neurons to two tests: (i) during choice over zero-  
 338 bundle; both rewards were set to zero in one bundle, and the animal unfailingly chose the  
 339 alternative, non-zero bundle; (ii) during choice between two non-zero bundles; at least one reward  
 340 was set to non-zero in both bundles, and the animal chose either bundle.

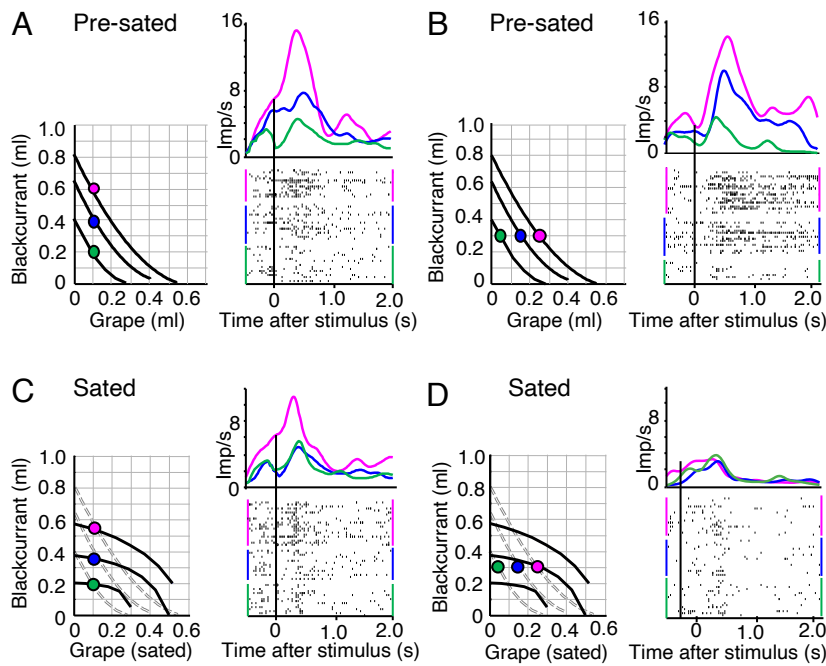
341 All satiety-tested neuronal responses followed the basic scheme of ICs: monotonic increase  
 342 with bundles placed on different ICs (testing bundles with different utility), and insignificant  
 343 response variation with bundles positioned along same ICs (testing equally preferred bundles with  
 344 equal utility) (Pastor-Bernier et al. 2019). We assessed these characteristics with a combination of  
 345 multiple linear regression (Eq. 3), Spearman rank-correlation, and 2-way Anova (see Methods). All  
 346 tested responses belonged to the subgroup of OFC neurons that were sensitive to multiple rewards  
 347 and coded the value of the bundle the animal chose ('chosen value', as defined by Eqs. 4 and 5). Our  
 348 task design aimed for maximal similarity between the two choice options and therefore used  
 349 quantitative bundle stimuli that were visually not unequivocally identifiable; therefore, we could not  
 350 test object value or offer value that indicate the value of an identifiable choice option.

351 We tested the influence of on-going reward consumption during the recording period of  
 352 individual neurons, which allowed us to compare responses in non-sated vs. sated states for the  
 353 same neuron, as defined by IPs inside vs. outside 95% CIs, respectively (Figure 1D, green zone). As  
 354 these tests required several tens of minutes with each neuron, neurons not coding chosen value were  
 355 not further investigated. Our test involved two bundle placements that considered the IC properties:  
 356 variation of blackcurrant juice while holding grape juice constant, and variation of grape juice while  
 357 holding blackcurrant juice constant. Comparison of the x-y plots between the pre-sated state (Figure  
 358 4A and B) and the sated state (C and D) illustrates this test scheme. The IC flattening with satiety  
 359 moved the bundle positions relative to the ICs substantially for grape juice variation (compare B  
 360 and D) but very little for blackcurrant juice variation (compare A with C). Thus, tests following this  
 361 design should be sensitive for detecting neuronal changes with satiety.

### 363 **Single-neuron value-coding follows IC changes**

364 At the beginning of daily testing, neuronal responses during choice over zero-bundle followed  
 365 monotonically the increase of both bundle rewards, confirming value coding (Figure 4A, B). The  
 366 ICs changed with on-going reward consumption. Despite the change, bundles aligned according to  
 367 increasing blackcurrant juice were still positioned on different ICs, and the neuronal responses  
 368 correspondingly continued to distinguish reward value (although in this case only between the top  
 369 two utilities) (Figure 4C; red vs. blue-green). By contrast, as the ICs flattened and became concave,  
 370 the three physically unaltered bundles aligned with increasing grape juice were now positioned on  
 371 or near only one IC (Figure 4D, left), indicating similar utility despite increasing grape juice. The  
 372 IC concavity indicated that the animal was only ready to give up meaningful amounts of  
 373 blackcurrant juice (on which it was less sated) when higher amounts of grape juice were offered  
 374 (right, descending part of IC). Correspondingly, OFC responses failed to vary with grape juice  
 375 amounts on the flat part of the sated IC (Figure 4D, right), and the response peak for the largest  
 376 grape juice amount dropped by 75%. Thus, with on-going consumption of both juices, neuronal  
 377 coding was maintained but reflected the utility reduction of grape juice relative to blackcurrant juice  
 378 indicated by the corresponding IC changes.

379



380  
381

382 **Figure 4. Response change in single OFC neuron reflecting relative reward-specific satiety**

383 (A) Monotonic response increase across three indifference curves (IC) with increasing blackcurrant juice  
384 before satiety during choice over zero-bundle. Each colored dot indicates a bundle with specific amounts of  
385 blackcurrant and grape juice located on a specific IC. Responses varied monotonically and significantly  
386 across ICs with increasing blackcurrant juice (grape juice remained constant) ( $P = 0.0053$ ,  $F = 8.88$ , 36  
387 trials; 1-way Anova).

388 (B) As (A) but significant response variation with grape juice across ICs (blackcurrant juice remained  
389 constant) ( $P = 1.97141 \times 10^{-6}$ ,  $F = 39.73$ , 25 trials). Same colors as in (A).

390 (C) After on-going consumption of both bundle rewards while recording from same neuron: lack of effect for  
391 unsated blackcurrant juice. Despite IC change, the three bundles remained on their three original and  
392 separate ICs, and neuronal coding of blackcurrant juice remained significant ( $P = 0.0029$ ,  $F = 10.28$ , 36  
393 trials). Note 29% reduction of peak response, from 15.5 to 11 impulses/s (red), and indiscriminate responses  
394 between intermediate and low bundles. Grey dotted lines repeat the ICs before satiety shown in (A).

395 (D) Neuronal response change for sated grape juice: response reduction by 75% (from 15.2 to 3.8 imp/s at  
396 peak, red), and loss of significant variation ( $P = 0.1116$ ,  $F = 2.68$ , 34 trials). After the consumption-induced  
397 slope and curvature change of the ICs (from convex to concave), the three physically unchanged bundles lie  
398 now on or close to the same, intermediate IC, indicating similar utility among them and reflecting satiety for  
399 grape juice. Dotted ICs are from pre-sated state. Thus, while continuing to code reward value (C), the  
400 responses followed the satiety-induced IC change.

401

402 The same consumption-induced neuronal changes occurred in choice between two non-zero  
403 bundles (Figure S2). Bundles varying only in blackcurrant juice remained on similarly increasing  
404 ICs as before; correspondingly, the chosen value OFC responses continued to increase with  
405 blackcurrant juice, confirming basically unaltered coding of blackcurrant juice (Figure S2A, C). By  
406 contrast, the three physically unaltered bundles varying only in grape juice were now on lower and  
407 narrower spaced ICs, indicating lower and less different values; the neuronal responses decreased  
408 correspondingly and became less differential (Figure S2B, D; red, blue, green). Further, the  
409 responses to the physically unaltered bundle whose position had changed from intermediate to  
410 highest IC (hollow blue) now dominated all other responses (Figure S2D right, dotted blue line).  
411 Finally, before satiety the bundle containing only 0.6 ml blackcurrant juice had similar utility as the  
412 bundle with only 0.4 ml grape juice (Figure S2B; hollow and solid blue dots on same IC), and  
413 correspondingly drew similar neuronal responses (dotted and solid blue lines), whereas with satiety

414 the physically same two bundles were positioned on different ICs (Figure S2D; hollow vs. solid  
 415 blue dot) and correspondingly drew different responses (dotted vs. solid blue line). Thus, the  
 416 differential neuronal response changes with on-going reward consumption occurred irrespective of  
 417 choice over zero-bundle or choice between two non-zero bundles.

418 Taken together, OFC neurons continued to code reward value with on-going reward  
 419 consumption. The responses continued to discriminate well the amount of blackcurrant juice whose  
 420 utility had changed relatively less (Figures 4A, 4C, S2A, S2C) but were altered for grape juice  
 421 whose relative utility had dropped more (Figures 4B, 4D, S2B, S2D). The altered OFC signals  
 422 reflected the reward-specific relative utility change induced by on-going consumption as inferred  
 423 from the altered ICs.

424

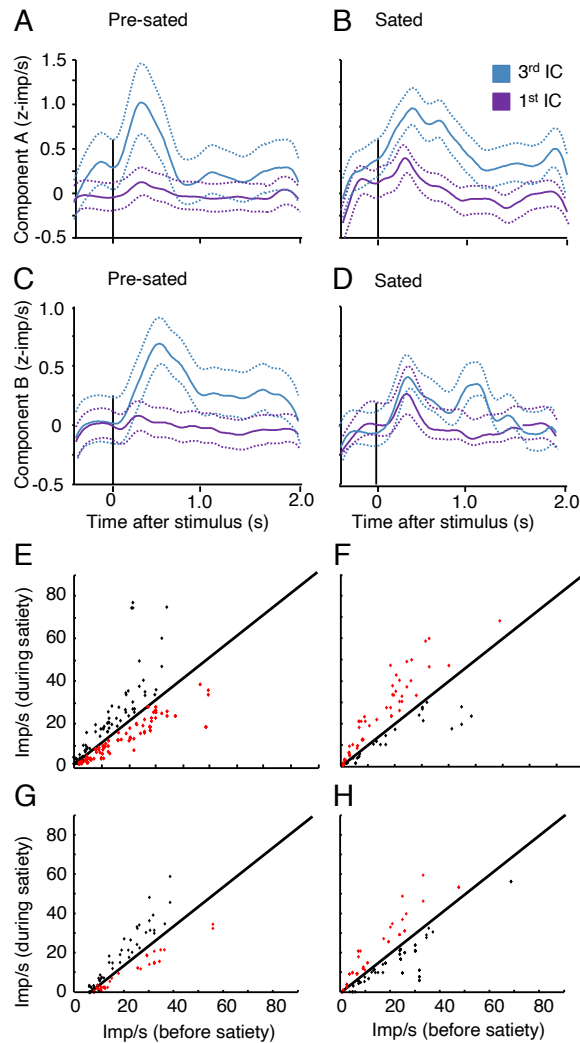
### 425 **Neuronal population**

426 We investigated the effects of on-going reward consumption in a total of 272 task-related OFC  
 427 neurons in area 13 at 30-38 mm anterior to the interaural line and lateral 0-19 mm from the midline;  
 428 these neurons were parts of the population reported previously (Pastor-Bernier et al., 2019).  
 429 Responses in 98 of these OFC neurons coded chosen value (defined by Eqs. 4 and 5) and followed  
 430 the IC scheme in any of the four task epochs (Bundle stimulus, Go, Choice or Reward) during  
 431 choice over zero-bundle or choice between two non-zero bundles (Table 1). Of the 98 chosen value  
 432 neurons, 82 showed satiety-related changes with bundles composed of blackcurrant juice  
 433 (component A) and grape juice, water or mango juice (component B) (Table 2).

434 We tested averaged z-scored neuronal population responses with the same scheme of bundle  
 435 alignment on ICs as with single neurons; the scheme is shown in Figures 4 and S2. Bundles aligned  
 436 with blackcurrant juice (component A) remained on the same three ICs during satiety; by contrast,  
 437 with consumption-induced IC flattening, bundles aligned with grape juice, water or mango juice  
 438 (component B) that were on different ICs before satiety were now very close to a single,  
 439 intermediate IC with little utility variation (see left x-y maps in Figures 4 and S2). The population  
 440 of 101 positive value coding responses in 31 neurons continued to vary with blackcurrant juice  
 441 amount during satiety in any task epoch (Bundle stimulus, Go, Choice or Reward), although with  
 442 12% peak reduction (Figure 5A, B). By contrast, neuronal coding of reward amounts of component  
 443 B in the same neurons went from significant before satiety to insignificant during satiety, with 43%  
 444 peak reduction (Figure 5C, D). Thus, the neuronal population responses showed similar alterations  
 445 as single neuron responses.

446 Numeric quantification of individual responses demonstrated satiety-induced significant  
 447 response reduction with positive value coding neurons (higher response with higher value) and  
 448 significant response increase with negative (inverse) coding neurons (lower response with higher  
 449 value) during choice over zero-bundle (Figure 5E and F, red) and during choice between two non-  
 450 zero bundles (Figure 5G and H, red; Table 2). These responses changes reflected the differential  
 451 reduction in reward value from on-going reward consumption. By contrast, a minority of neurons  
 452 showed either inverse changes that were difficult to reconcile with the changes in value (black in  
 453 Figure 5E-H), or no significant changes at all.

454



455  
456

457 **Figure 5. Population responses**

458 (A) - (D) Averaged z-scored population responses from 31 positive coding neurons showing response  
459 reduction during satiety. Each part shows responses to bundles on lowest and highest of three indifference  
460 curves (IC) during choice over zero-bundle. Data are from choice over zero-bundle, both animals, four  
461 bundle types (component A: blackcurrant juice, component B: grape juice, water or mango juice). The  
462 response differences between lowest and highest ICs were statistically significant both before satiety ( $P =$   
463  $1.53862 \times 10^{-5}$ ,  $F = 19.28$ , 1-way Anova) and during satiety ( $P = 2.96646 \times 10^{-16}$ ,  $F = 72.18$ ), but degraded  
464 and lost statistical significance with component B (before satiety:  $P = 4.39918 \times 10^{-16}$ ,  $F = 73.24$ ; during  
465 satiety:  $P = 0.6796$ ,  $F = 0.17$ ). Dotted lines show  $\pm 95\%$  confidence intervals.

466 (E) Response changes in positively coding neurons in any of four task epochs (Bundle stimulus, Go, Choice  
467 and Reward; Table 2) during choice over zero-bundle. Red: significant response decrease in population  
468 reflecting satiety-induced value reduction ( $P = 7.15 \times 10^{-4}$ ; 101 responses in 31 neurons; 1-tailed t-test).  
469 Black: significant response increase ( $P = 0.0014$ ; 69 responses in 21 neurons). Imp/s: impulses/second).  
470 (F) As (E) but for negative (inverse) value coding neurons. Red: significant response increase reflecting  
471 satiety-induced value reduction ( $P = 0.0013$ ; 54 responses in 15 neurons). Black: insignificant response  
472 decrease ( $P = 0.1274$ ; 33 responses in 14 neurons).

473 (G) As (E) but for choice between two non-zero bundles. Red: response decrease ( $P = 0.0156$ ; 54 responses  
474 in 16 neurons; 1-tailed t-test). Black: response increase ( $P = 0.0101$ ; 57 responses in 16 neurons). Imp/s:  
475 impulses/second).

476 (H) As (F) but for choice between two non-zero bundles. Red: significant response increase ( $P = 0.0242$ ; 31  
477 responses in 9 neurons). Black: insignificant response decrease ( $P = 0.1939$ ; 36 responses in 14 neurons).

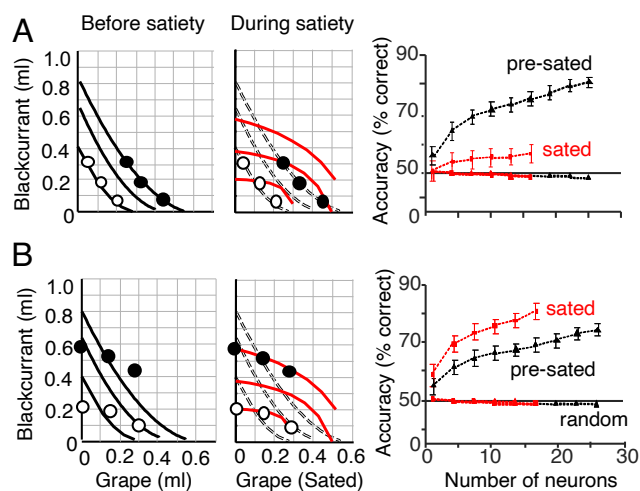
478

## 479 **Neuronal satiety-induced changes indicated by classification accuracy**

480 Next we used a neuronal classifier as another means for demonstrating how much on-going reward  
 481 consumption changed neuronal reward coding. We first established the accuracy with which  
 482 neuronal responses distinguished bundles on different ICs before satiety set in; satiety was defined  
 483 by IPs exceeding their CIs (Figure 1D). Then we tested the accuracy with which initial neuronal  
 484 bundle responses distinguished the physically same bundles after on-going reward consumption had  
 485 changed the ICs. If the neuronal responses had changed substantially with on-going reward  
 486 consumption, classification accuracy should be low when a classifier trained on bundle responses  
 487 before satiety was tested for bundle discrimination after satiety. To this end, we trained a support  
 488 vector machine (SVM) classifier on neuronal responses to randomly selected bundles positioned on  
 489 the lowest and highest of three ICs, respectively.

490 The classifier trained on neuronal responses to bundle stimuli before satiety showed decent  
 491 bundle discrimination with as few as five neurons during choice over zero-bundle; classifier  
 492 performance was intuitively meaningful as it increased with added neurons (Figure 6A). However,  
 493 accuracy dropped dramatically when the same classifier trained before satiety was tested for bundle  
 494 distinction between different ICs during satiety; the maintained accuracy increase with added  
 495 neurons demonstrated valid classification. Inversely, accuracy was high when training and testing  
 496 the classifier during satiety (Figure 6B), but lower when training during satiety and testing for  
 497 bundle distinction before satiety, thus confirming the neuronal changes with satiety.

498 These accuracy differences were seen during choice over zero-bundle with neuronal responses  
 499 to Bundle stimuli (Figure 6) and during the Go epoch (Figure S3A), but not during Choice and  
 500 Reward epochs (Figure S3B, C). The changes were not explained by baseline changes during the 1 s  
 501 Pretrial control epoch (Figure S3D). Similar substantial accuracy differences were seen in choice  
 502 between two non-zero bundles during Bundle stimuli, Go epoch and Choice epoch but not during  
 503 the Reward epoch (Figure S3E-H), again not explained by baseline changes (Figure S3I). The  
 504 accuracy differences were consistent across on-going consumption steps (Figure S3J).  
 505



506

### 507 **Figure 6. Bundle classification demonstrates satiety-induced change of neuronal value coding**

508 (A) Bundle classification by support vector machine using neuronal responses to stimuli of bundles  
 509 positioned on the lowest and highest indifference curve, respectively (choice over zero-bundle). The  
 510 classifier was trained on neuronal responses before satiety and tested for bundle distinction before satiety  
 511 (black) and during satiety (red). Left: identical bundle positions on two-dimensional map but IC change with  
 512 on-going consumption, indicating satiety-induced relative utility change (red). Right: classifier accuracy  
 513 increase with neuron numbers before satiety (black), but drop when tested for bundle distinction during  
 514 satiety (red). Error bars indicate standard errors of the mean (SEM).

515 (B) As (A), but reverse order: classifier trained on neuronal responses during satiety and tested before  
 516 satiety.

517

518 In demonstrating substantial accuracy changes, these tests suggested that the neuronal  
 519 responses followed the substantial IC changes that reflected the utility changes from on-going  
 520 reward consumption indicative of satiety.

521

### 522 **Neuronal satiety changes with single-reward bundles**

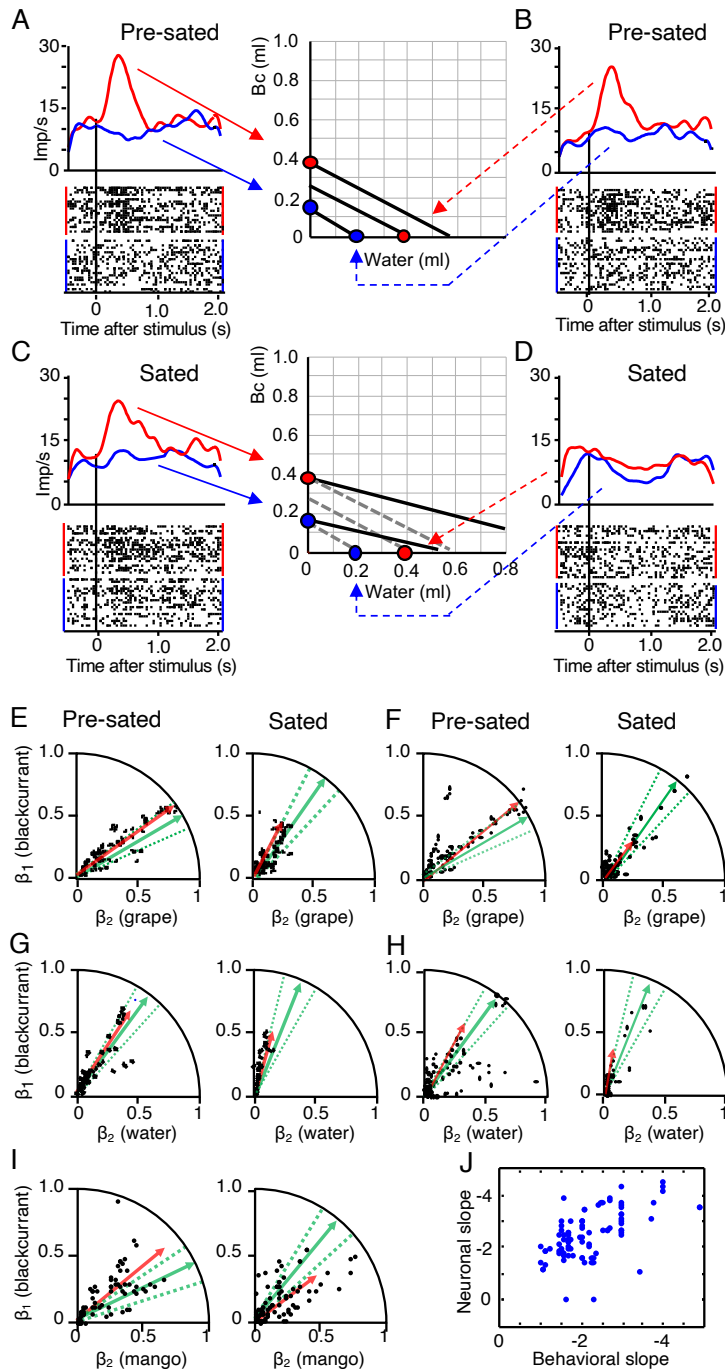
523 Using choice options with two reward components differs in several ways from previous studies  
 524 using single rewards (Tremblay & Schultz 1999; Padoa-Schioppa & Assad 2006) and thus requires  
 525 controls and additional analyses. We used the same two visual component stimuli but set only one,  
 526 but different, reward in each bundle to a non-zero amount, which positioned the bundles graphically  
 527 along the x-axis and y-axis but not inside the IC map (anchor trials; Figure S1B). These degenerated  
 528 bundles were equivalent to single-reward choice options tested earlier (Padoa-Schioppa & Assad  
 529 2006).

530 First we used single-reward bundles for confirming the results with our two-component  
 531 bundles. The responses of the neuron shown in Figure 7A, B distinguished both rewards during  
 532 choice over zero-bundle before satiety. With on-going consumption of both rewards, the ICs  
 533 flattened, preserving the blackcurrant juice positions on the ICs but changing the physically  
 534 unchanged position of the two water amounts relative to the ICs (Figure 7C, D). The neuron kept  
 535 discriminating blackcurrant juice amounts during satiety (Figure 7C). However, with the satiety-  
 536 induced IC change, the large water amount was now positioned much more below the highest IC  
 537 than before (Figure 7D, red on x-axis) and on about the same IC as the small blackcurrant amount  
 538 (blue on y-axis). Correspondingly, the neuronal activity with the large water amount lost its peak  
 539 (reduction by 50%) and was now very similar to the activity with the small blackcurrant amount  
 540 (Figure 7C, D, red dotted vs. blue solid arrows). Further, the position of the small water amount was  
 541 now below its original IC (blue on x-axis), and the neuron, with its lost response, failed to  
 542 distinguish between the two water amounts. Thus, the neuronal changes with single-reward bundles  
 543 followed the satiety-induced IC changes, demonstrating that the neuronal satiety changes reported  
 544 above occurred also with single rewards (degenerated bundles).

545 Next, we used single-reward bundles to quantify neuronal response changes with on-going  
 546 reward consumption in relation to utility changes inferred from behavioral choices. We established  
 547 vector plots that display the ratio of reward weights ( $\beta$ 's) for behavioral choice (Eq. 1a; Figure 7E-I,  
 548 green) and z-scored neuronal population responses (Eq. 3; red). The inequality of utilities of the two  
 549 rewards was manifested as deviation of these vectors from the diagonal. On-going reward  
 550 consumption increased the elevation angle of the behavioral vector, indicating loss of utility for  
 551 component B (grape juice, water or mango juice) relative to component A (blackcurrant juice). The  
 552 neuronal vector changed correspondingly (Figure 7E-I, green vs. red). For example, during choice  
 553 of the bundle (blackcurrant juice, grape juice) over zero-reward bundle, the elevation angle of the  
 554 behavioral vector increased from 40 deg before satiety to 65 deg during satiety, and the neuronal  
 555 population vector increased correspondingly from 35 deg to 62 deg (Figure 7E, green, red).  
 556 Similarly, during choice between two non-zero bundles, the behavioral vector increased from 40  
 557 deg to 52 deg and the neuronal vector increased correspondingly from 38 deg to 45 deg (Figure 7F).  
 558 Further, the shorter neuronal vectors during satiety indicated general reduced responding (red).  
 559 Bundles containing water or mango juice showed similar changes (Figure 7G-I). Thus, both before  
 560 and during satiety, the neuronal vectors (red) were within the CIs of the behavioral vectors (green),  
 561 indicating intact neuronal value coding that followed the utility changes with on-going reward  
 562 consumption.

563 In addition to the vector analysis, IC slopes confirmed the close neuronal-behavioral  
 564 correspondence during satiety, with satiety being defined by the IPs exceeding the initial, pre-sated  
 565 IPs (Figure S1A, E). As estimated from regression coefficient ratios ( $-\beta_2 / \beta_1$ ) (Eq. 3) and ( $-b / a$ )  
 566 (Eq. 1), the slopes of the linear neuronal ICs of single-reward bundles correlated well with the  
 567 slopes of linear behavioral ICs (Figure 7J). These results from testing single-reward bundles with  
 568 on-going reward consumption compared well with the results from the earlier OFC study on single  
 569 rewards with spontaneously varying subjective reward value (Padoa-Schioppa & Assad 2006).

570 Taken together, the population changes indicated the influence of relative, reward-specific  
 571 satiety on neuronal reward value coding. They confirmed the single-neuron changes with single-  
 572 reward bundles (Figure 7A-D) and multi-reward bundles (Figures 4, S2).  
 573



574  
575

576 **Figure 7. Reward-specific satiety with single-reward bundles**  
 577 (A-D) Responses of same single neuron before and during satiety. Each bundle contained specific non-zero  
 578 amounts of only blackcurrant juice or only water (colored dots on indifference curves, ICs) and was tested  
 579 during choice over zero-bundle.  
 580 (A) Significant response increase across two ICs with increasing blackcurrant juice (Bc) before satiety  
 581 (water remained zero) (red vs. blue;  $P = 0.0091$ ,  $F = 6.92$ , 23 trials; 1-way Anova).  
 582 (B) As (A) but significant response variation with increasing water across two ICs (blackcurrant juice  
 583 remained zero) ( $P = 0.0113$ ,  $F = 7.32$ , 31 trials). Same colors as (A).

584 (C) Despite IC flattening after on-going reward consumption, the two bundles with blackcurrant juice  
 585 variation remained on the same two ICs, and the neuronal response variation remained significant ( $P =$   
 586  $0.002$ ,  $F = 11.04$ , 40 trials), and the peak response was only slightly reduced (red). Dotted ICs are from pre-  
 587 sated state.

588 (D) IC flattening after on-going reward consumption indicates relative utility reduction of water. The two  
 589 unchanged bundles with water variation were now located below and at the IC. The neuronal response was  
 590 substantially reduced by 50% (red) and had lost significant variation ( $P = 4337$ ,  $F = 0.64$ , 40 trials).  
 591 Further, the large-water bundle (dashed red line) elicited now a similar response as the low-blackcurrant  
 592 bundle that is now located on the same IC (solid blue line). Thus, while continuing to code reward value (C),  
 593 the responses followed the satiety-induced IC change.

594 (E) Vector plots for behavioural choice of bundle (blackcurrant juice, grape juice) over zero-bundle (green)  
 595 and corresponding  $z$ -scored neuronal population responses (black, red). Neuronal vector slopes were 35 deg  
 596 before satiety and 62 deg during satiety, using all significantly positive and normalized negative (inverse)  
 597 coding responses from all four task epochs; all included responses followed the IC scheme. Dots refer to  
 598 neuronal responses, vectors represent averages from behavioral choices (green; dotted lines: 95%  
 599 confidence intervals) and neuronal responses (red), based on Eqs. 1a and 3, respectively (see Methods).  
 600 Neuronal slope regression coefficients ( $\beta$ 's) on axes refer to Eq. 3.

601 (F) As for (C) but for choice between two non-zero bundles. Neuronal vector slopes were 38 deg before and  
 602 45 deg during satiety.

603 (G), (H) As (E, F) but for bundle (blackcurrant juice, water).

604 (I) As (E) but for bundle (blackcurrant juice, mango juice).

605 (J) Correlation between rectified neuronal and behavioral IC slopes ( $\beta$ 's from Eqs. 3 and 1a, respectively)  
 606 during satiety in all tested neurons ( $\rho = 0.604$ ;  $P = 8 \times 10^{-6}$ , Pearson correlation;  $\rho = 0.595$ ,  $P = 2 \times$   
 607  $10^{-5}$ , Spearman rank-correlation;  $N = 90$  responses during choice between two non-zero bundles).

608

## 609 Discussion

610

611 This study tested binary choice between bundles of two rewards and found response changes in  
 612 OFC reward neurons that suggested a differential loss of reward utility indicative of relative reward-  
 613 specific satiety from on-going reward consumption. The choices were captured by graphic ICs that  
 614 represented the relative utilities of the two bundle rewards in a conceptually rigorous manner. The  
 615 ICs changed in an orderly and characteristic manner with on-going reward consumption, without  
 616 requiring unnatural reward bolus administration (Figures 1, 2, S1). The ICs flattened progressively  
 617 and showed gradual curvature changes from convexity to concavity, which indicated gradual utility  
 618 loss for one bundle reward (blackcurrant juice, plotted on the y-axis) relative to the other bundle  
 619 reward (all other bundle rewards except peach juice, x-axis). This IC change suggested that the  
 620 animal became increasingly reluctant to give up blackcurrant juice for the same increment of the  
 621 other reward. The specific and asymmetric IC changes make alternative explanations unlikely, such  
 622 as passage of time, general satiety, loss of motivation, or proximity of return to home cage, all of  
 623 which would have affected all rewards in a similar manner. Licking behavior supported the notion  
 624 of differential reward satiety in a mechanism-independent manner (Figure 3).

625 Our preceding study had established neuronal chosen value responses in OFC that were  
 626 sensitive to multiple rewards and followed the animal's rational choice of two-reward bundles,  
 627 including completeness, transitivity and independence from option set size (Pastor-Bernier et al.,  
 628 2019). The current study tested the effects of on-going reward consumption during the recording  
 629 period of individual neurons. We found OFC value responses that matched the consumption-  
 630 induced IC changes. The responses became weaker for the more devalued reward, as indicated by  
 631 slope and curvature changes of ICs (Figures 4, 5, S2). Most impressively, neuronal responses failed  
 632 to distinguish between bundles that had landed on the flat parts of ICs because of the ICs' curvature  
 633 change to concave (Figure 4D). Classifiers predicting bundle discrimination from neuronal  
 634 responses confirmed accurate reward value coding both before and during satiety and demonstrated  
 635 the substantial nature of the neuronal changes (Figures 6, S3). Neuronal response vectors of

636 conventional single-reward choice options correlated well with behavioral choice vectors; these  
637 correlations were maintained with the utility change from on-going reward consumption (Figure 7).  
638 Taken together, these particularly sensitive reward utility tests, informed by Revealed Preference  
639 Theory, demonstrate good correlation between OFC responses and the differential utility alterations  
640 induced by on-going reward consumption. As the physical reward properties did not change with  
641 satiety, these results also confirm the subjective value (utility) coding of OFC neurons demonstrated  
642 with choices between two-component bundles (Pastor-Bernier et al., 2019) and single rewards  
643 (Padoa-Schioppa & Assad, 2006).

644 The observed increase in consumption of sated liquids like water (Figure 3H) seemed to  
645 contradict earlier findings and the general intuition that satiety would rather reduce consumption of  
646 rewards on which an animal is sated (Rolls et al. 1989; Critchley & Rolls 1996). Differences in  
647 study design might explain these discrepancies. When an animal has the choice between a sated and  
648 a non-sated reward, or the choice between accepting and not accepting a reward, it would naturally  
649 prefer the non-sated reward. This was the case in the cited earlier studies. By contrast, in our study,  
650 the animal chose between two bundles that each had two differently sated rewards. As the animal  
651 was still interested to obtain the less sated bundle reward, it would inadvertently also receive the  
652 other, more sated reward that was a part of the bundle. The animal had no control over the setting of  
653 the Reference Bundle against which it would choose the alternative bundle. At the IP, the animal  
654 had the choice to give up some of the non-sated reward in order to receive more of the sated reward.  
655 If the animal had still a limited interest in the less sated reward, maybe because it was still  
656 somewhat thirsty, it might give up a limited amount in order to receive a lot more of the other  
657 reward (as long as it would not outrightly reject it, which was not the case). This trade-off was  
658 indicated by the increasing IC concavity with on-going consumption, which demonstrated that  
659 really large amounts of the more devalued Reward B were required for giving up the less devalued  
660 Reward A (Figures 1E, 2, S1D). Outright rejection of Reward B would be represented not by a  
661 downward sloped IC but by an upward sloped IC, which had been observed with lemon juice,  
662 yoghurt and saline (Pastor-Bernier et al., 2017) but not with the currently used rewards; such  
663 upward sloped ICs indicate that an animal needed to be 'bribed' with more reward for accepting  
664 these normally rejected rewards. By contrast, in the current satiety experiment, the animal  
665 inadvertently consumed more of the sated reward during satiety compared to before, and the  
666 maintained downward IC slope indicated that the animal was not entirely averse to the sated reward.

667 The current study of systematically altered reward value coding with reward-specific satiety  
668 builds on previous studies on monkey OFC neurons that investigated satiety in a more basic  
669 manner. There are notably the studies from Rolls' laboratory in which monkeys were presented with  
670 syringes or tubes containing various fruit juices; rating scales were used to assess behavioral  
671 acceptance or rejection of these juices after bolus administration (Rolls et al. 1989; Critchley &  
672 Rolls 1996). The studies report OFC neurons that responded to several juices and lost the responses  
673 only for the particular juice on which the animal was sated. The response reduction with sensory-  
674 specific satiety in OFC contrast with Rolls' studies on earlier stages of the gustatory system,  
675 including the nucleus of the solitary tract, the frontal opercular taste cortex, and the insular taste  
676 cortex, where no such satiety-related changes were found (Yaxley et al. 1985; Yaxley et al. 1988;  
677 Rolls et al. 1988). However, it is unknown whether the studied OFC neurons coded subjective  
678 reward value inferred from choices in the absence of satiety or covaried with other crucial aspects  
679 of subjective reward value, such as reward amount and behavioral preference that formed the basis  
680 for our study. A subsequent study with bolus water reward administration found even stronger  
681 general satiety effects in ventromedial prefrontal cortex compared to OFC (Bouret & Richmond,  
682 2010), suggesting widespread satiety effects in the ventral frontal cortex. Our results are compatible  
683 with the relationship between spontaneous choice variations and chosen value coding in monkey  
684 OFC (Padoa-Schioppa & Assad 2006); the choice variations likely reflected changes in thirst level  
685 that were synonymous with satiety variations during the course of each day's experimentation.  
686 These value changes were instrumental in distinguishing subjective value coding from the coding of  
687 purely physical properties during economic choice. Thus, the current experiment brings together a

688 number of heterogeneous arguments in favor of OFC coding of subjective value and presents a  
 689 conceptually coherent argument for economic utility coding according to Revealed Preference  
 690 Theory.

691 While reward-specific satiety concerns the specific utility of individual rewards, on-going  
 692 consumption induces also a reduction of general reward value manifested as changes in arousal,  
 693 attention and motivation. General satiety effects cannot be distinguished from reward-specific  
 694 satiety when testing only a single reward, and the effects may be attributed to loss of motivation, as  
 695 in the case of reduced dopamine responses in mice that received food pellets for extended periods of  
 696 time (Rossi et al., 2013). The loss of motivation may be associated with a loss of pleasure and  
 697 development of aversion; neural indices may consist of reduced human midbrain responses, as  
 698 shown with on-going consumption of Swiss chocolate (Small et al., 2001). In our results, the shorter  
 699 neuronal population vectors might indicate an effect of general satiety on neuronal responses  
 700 (Figure 7E-I), in addition to the reward-specific satiety suggested by the changes in vector angle.  
 701 However, general satiety cannot explain our asymmetric neuronal changes that correlate with  
 702 relative reward-specific utility changes.

703

## 704 **Materials and Methods**

705

706 The study used the same 2 male adult rhesus monkeys as previously (Pastor-Bernier et al.,  
 707 2019) and was licensed by the UK Home Office (for details, see Supplementary Information). The  
 708 animals chose between two bundles that contained the same two rewards with independently  
 709 varying amounts. We estimated psychophysically multiple choice indifference points (IP; Figure  
 710 1D, S1A, E) to which we fitted indifference curves (IC) along which all bundles were equally  
 711 preferred, using a hyperbolic function  $d$ :

712

$$713 \quad d = ay + bx + cxy \quad (\text{Eq. 1})$$

714

715 with  $y$  and  $x$  as milliliter amount of Rewards A and B (Figures 1C, E, S1B, D, F),  $a$  and  $b$  as  
 716 weights of the influence of the two Reward amounts, and  $c$  as curvature. Eq. 1 can be equivalently  
 717 re-written as regression in analogy to the regression used for analysing neuronal responses:

718

$$719 \quad y = \beta_0 + \beta_1A + \beta_2B + \beta_3AB + \varepsilon \quad (\text{Eq. 1a})$$

720

721 with  $A$  and  $B$  as milliliter amount of Reward A (plotted at  $y$ -axis) and Reward B ( $x$ -axis),  
 722 respectively,  $\beta_0$  as offset coefficient,  $\beta_1$  and  $\beta_2$  as behavioral regression coefficients, and  $\varepsilon$  as  
 723 compound of errors  $\text{err}_0, \text{err}_1, \text{err}_2, \text{err}_3$  for offset and regressors 1-3.

724 To test whether the animal's choice reflected the amount of the bundle rewards during satiety,  
 725 rather than other, unintended variables such as spatial bias, we used the logistic regression:

726

$$727 \quad P(V) = \beta_0 + \beta_1CT + \beta_2RA + \beta_3RB + \beta_4VA + \beta_5VB + \beta_6CL + \beta_7MA + \beta_8MB + \varepsilon \quad (\text{Eq. 2})$$

728

729 with  $P(V)$  as probability of choice of Variable Bundle,  $\beta_0$  as offset coefficient,  $\beta_1 - \beta_7$  as  
 730 correlation strength (regression slope) coefficients indicating the influence of the respective  
 731 regressor,  $CT$  as trial number within block of consecutive trials,  $RA$  as amount of Reward A of  
 732 Reference Bundle,  $RB$  as amount of Reward B of Reference Bundle,  $VA$  as amount of Reward A of  
 733 Variable Bundle,  $VB$  as amount of Reward B of Variable Bundle,  $CL$  as choice of any bundle  
 734 stimulus presented at the left,  $MA$  as consumed amount of Reward A,  $MB$  as consumed amount of  
 735 Reward B, and  $\varepsilon$  as compound error for offset and all regressors.

736

737 Following behavioral training and surgical preparation for single neuron recordings, we  
 738 identified neuronal task relationships with the paired Wilcoxon-test. We identified changes of task-  
 739 related neuronal responses across ICs with a linear regression:

$$y = \beta_0 + \beta_1 A + \beta_2 B + \beta_3 AB + \varepsilon \quad (\text{Eq. 3})$$

with  $y$  as neuronal response in any of the four task epochs, measured as impulses/s and z-scored normalized to the Pretrial control epoch of 1.0 s,  $A$  and  $B$  as milliliter amounts of Reward A (plotted at y-axis) and Reward B (x-axis), respectively,  $\beta_0$  as offset coefficient,  $\beta_1$  and  $\beta_2$  as neuronal regression coefficients, and  $\varepsilon$  as compound error. In addition, all significant neuronal response changes across ICs identified by Eq. 3 needed to be also significant in a Spearman rank-correlation test ( $P < 0.05$ ).

To assess neuronal compliance with the two-dimensional IC scheme, we used a two-factor Anova on each task-related response that was significant for both regressors in Eq. 3. Neuronal responses following the IC scheme were significant across-ICs (factor 1:  $P < 0.05$ ) but insignificant within-IC (factor 2).

Chosen value (CV) was defined as:

$$CV = A + k_1 B \quad (\text{Eq. 4})$$

weighting parameter  $k_1$  served to adjust for differences in subjective value between rewards  $A$  and  $B$ , such that the quantity of Reward  $B$  entered the regression on a common-currency scale defined by Reward  $A$ . We assessed neuronal coding of chosen value in all neurons that followed the revealed preference scheme, using the following regression:

$$y = \beta_0 + \beta_1 CV + \beta_2 UCV + \varepsilon \quad (\text{Eq. 5})$$

with  $UCV$  as value of the unchosen option that was not further considered here, and  $\varepsilon$  as compound error.

## References

- Bouret, S., and Richmond, B.J. (2010). Ventromedial and orbital prefrontal neurons differentially encode internally and externally driven motivational values in monkeys. *J Neurosci* 30: 8591-8601.
- Critchley, H.D., and Rolls, E.T. (1996). Olfactory neuronal responses in the primate orbitofrontal cortex: analysis in an olfactory discrimination task. *J. Neurophysiol.* 75, 1659-1672.
- Dhar, R., & Novemsky, N. (2008). Beyond rationality: the content of preferences. *J Consum Psychol* 18, 175-178.
- Fisher, I. (1892). *Mathematical Investigations in the theory of value and prices*. Trans Connecticut Acad 9, 1-124.
- Gottfried JA, O'Doherty J, Dolan RJ (2003) Encoding predictive reward value in human amygdala and orbitofrontal cortex. *Science* 301, 1104-1107.
- Izquierdo A, Suda RK, Murray EA (2004). Bilateral orbital prefrontal cortex lesions in rhesus monkeys disrupt choices guided by both reward value and reward contingency. *J Neurosci* 24, 7540-7548.
- Kivetz, R., Netzer, O., & Schrift, R. (2008) The synthesis of preference: Bridging behavioral decision research and marketing science. *Journal of Consumer Research* 18, 179-186.
- Kobayashi, S., Pinto de Carvalho, O., and Schultz, W. (2010). Adaptation of reward sensitivity in orbitofrontal neurons. *J. Neurosci.* 30, 534-544.
- Knetsch, J. L. (1989). The endowment effect and evidence of nonreversible indifference curves. *Am Econ. Rev.* 79, 1277-1288.
- Kringelbach, M.L., O'Doherty, J., Rolls, E.T., and Andrews, C. (2003). Activation of the human orbitofrontal cortex to a liquid food stimulus is correlated with its subjective pleasantness. *Cereb. Cortex* 13, 1064-1071.
- Merrill, E. G., and Ainsworth, A. (1972). Glass-coated platinum-plated tungsten microelectrodes. *Med. Biol. Eng.* 10, 662-672.

- 793 Murray EA, Moylan EJ, Saleem KS, Basile BM, Turchi J (2015). Specialized areas for value  
794 updating and goal selection in the primate orbitofrontal cortex. *eLife* 4: e11695
- 795 Padoa-Schioppa, C. (2009). Range-adapting representation of economic value in the orbitofrontal  
796 cortex. *J. Neurosci.* 29, 14004-14014.
- 797 Pastor-Bernier, A., Stasiak, A., and Schultz, W. (2019). Orbitofrontal signals for two-component  
798 choice options comply with indifference curves of Revealed Preference Theory. *Nat. Comm.*  
799 10, 4885.
- 800 Pastor-Bernier, A., Plott, C.R., and Schultz, W. (2017). Monkeys choose as if maximizing utility  
801 compatible with basic principles of revealed preference theory. *Proc Natl AcadSci U S A.* 114,  
802 E1766-E1775.
- 803 Paxinos, G., Huang, X.-F. and Toga, A. W. (2000). *The Rhesus Monkey Brain in Stereotaxic*  
804 *Coordinates* (Academic Press, San Diego).
- 805 Payne, J. W., Bettman, J. R., & Schkade, D. A. (1999). Measuring constructed preferences: towards  
806 a building code. *J Risk Uncert* 19, 243-270.
- 807 Rolls, E.T., Sienkiewicz, Z.J., and Yaxley, S. (1989). Hunger Modulates the Responses to  
808 Gustatory Stimuli of Single Neurons in the Caudolateral Orbitofrontal Cortex of the Macaque  
809 Monkey. *Eur. J. Neurosci.* 1, 53-60.
- 810 Rolls, E.T., Scott, T.R., Sienkiewicz, Z.J., and Yaxley, S. (1988). The responsiveness of neurons in  
811 the frontal opercular gustatory cortex of the macaque monkey is independent of hunger. *J*  
812 *Physiol.* 397, 1-12.
- 813 Ross, M.A., Fan, D., Barter, J.W. and Yin, H.H. (2013). Bidirectional modulation of substantia  
814 nigra activity by motivational state. *PLoS ONE* 8: e71598.
- 815 Rudebeck PH, Saunders RC, Prescott AT, Chau, LS, Murray EA (2013). Prefrontal mechanisms of  
816 behavioral flexibility, emotion regulation and value updating. *Nat Neurosci* 16: 1140-1145.
- 817 Rustichini, A., Conen, K.E., Cai, X., Padoa-Schioppa, C. (2017). Optimal coding and neuronal  
818 adaptation in economic decisions. *Nat. Comm.* 8, 1208.
- 819 Samuelson, P. A. (1937). A note on measurement of utility. *Rev Econ Stud* 4, 155-161.
- 820 Samuelson, P. A. (1938). A note on the pure theory of consumer's behavior. *Economica* 5, 61-71.
- 821 Simonson, I. (2008). Will I like a "medium" pillow? Another look at constructed and inherent  
822 preferences. *J Consum Psychol* 18, 155-169.
- 823 Small, D.M., Zatorre, R.J., Dagher, A., Evans, A.C., and Jones-Gotman, M. (2001). Changes in  
824 brain activity related to eating chocolate: from pleasure to aversion. *Brain* 124, 1720-33.
- 825 Tremblay, L., and Schultz, W. (1999). Relative reward preference in primate orbitofrontal cortex.  
826 *Nature* 398, 704–708.
- 827 Tsutsui, K. I., Grabenhorst, F., Kobayashi, S. & Schultz, W. (2016). A dynamic code for economic  
828 object valuation in prefrontal cortex neurons. *Nat. Comm.* 7, 12554.
- 829 Warren, C., McGraw, A. P., & Van Boven, L. (2011). Values and preferences: defining preference  
830 construction. *WIREs Cogni Sci* 2, 193-205.
- 831 Yaxley, S., Rolls, E.T., Sienkiewicz, Z.J., and Scott, T.R. (1985). Satiety does not affect gustatory  
832 activity in the nucleus of the solitary tract of the alert monkey. *Brain Res.* 347, 85-93.
- 833 Yaxley, S., Rolls, E.T., and Sienkiewicz, Z.J. (1988). The responsiveness of neurons in the insular  
834 gustatory cortex of the macaque monkey is independent of hunger. *Physiol. Behav.* 42, 223-  
835 229.
- 836

837 **Table 1. Numbers of neurons tested with on-going reward consumption**

838

Bundle type	Choice over zero-bundle		Choice between two non-zero bundles	
	Neurons tested	IPs tested	Neurons tested	IPs tested
Blackcurrant, grape	21+11=32	28	7+12=19	38
Blackcurrant, water	20+13=33	39	22+12=34	58
Blackcurrant, mango	14+7=21	11	9+8=17	10
SUM	55+31=86	78	38+32=70	106

839

840 The bundle types (blackcurrant, grape) and (blackcurrant, water) were tested in Monkey A (81 and  
841 138 neurons, respectively), whereas bundle type (blackcurrant, mango) was tested in Monkey B (53  
842 neurons). Of these neurons, the neuron and response numbers given above coded chosen value (as  
843 identified by Eqs. 4 and 5) and followed the IC scheme, as defined previously (Pastor-Bernier et  
844 al., 2019): monotonic increase or monotonic decrease with bundles compared across ICs,  
845 insignificant response variation with bundles compared along individual ICs. Such neurons were  
846 recorded only during choice over zero-bundle (N = 28 neurons), only during choice between two  
847 non-zero bundles (N = 12 neurons), or both (N = 58 neurons) (total of 98 neurons). In table cells  
848 with multiple entries, the first two numbers refer respectively to positive and negative (inverse)  
849 relationships to increasing reward quantity, as inferred from the neuronal regression slope ( $\beta$ 's in  
850 Eq. 3). IP; bundle at choice indifference point at specific x-y coordinate.

851

852 **Table 2. Neuronal changes with on-going reward consumption**

853

Choice over zero-bundle						
Task epoch	Neurons tested	Neurons	Responses	Neurons	Responses	Neurons
		Response decreases		Response increases		No effects
Positive coding						
Bundle stimulus			30		21	
Go			28		17	
Choice			25		15	
Reward			18		16	
Subtotal	55	31	101	21	69	3
Negative coding						
Bundle stimulus			10		15	
Go			8		15	
Choice			8		11	
Reward			7		13	
Subtotal	31	14	33	15	54	2
Choice between two non-zero bundles						
Task epoch	Neurons tested	Neurons	Responses	Neurons	Responses	Neurons
		Response decreases		Response increases		No effects
Positive coding						
Bundle stimulus			16		16	
Go			15		15	
Choice			13		16	
Reward			10		10	
Subtotal	38	16	54	16	57	6
Negative coding						
Bundle stimulus			11		9	
Go			9		8	
Choice			8		6	
Reward			8		8	
Subtotal	32	14	36	9	31	9

854

855

856

857

858

859

860

This table includes data from chosen value responses, separated according to the four task epochs (Bundle stimulus, Go, Choice and Reward) and all bundles tested for satiety (component A: blackcurrant juice, component B: grape juice, water or mango juice). Positive coding refers to response increase with higher value before satiety, whereas negative coding refers to response decrease with higher value. Most neurons were tested both in choice over zero-bundle and in choice between two non-zero bundles.

861  
862 **Supplementary information for**  
863  
864 **Orbitofrontal cortex neurons code utility changes during natural reward consumption as**  
865 **correlates of relative reward-specific satiety**

866  
867 **Alexandre Pastor-Bernier, Arkadiusz Stasiak and Wolfram Schultz\***

868  
869 Corresponding author: Wolfram Schultz  
870 Email: Wolfram.Schultz@Protonmail.com

871  
872 This Supplementary Information includes:  
873     Supplementary Methods  
874     Supplementary Figures S1 to S3 and their legends

875  
876 **SI METHODS**

877 **Animals**

878 Two adult male macaque monkeys (*Macaca mulatta*; Monkey A, Monkey B), weighing 11.0 kg and  
879 10.0 kg, respectively, were used in these experiments that had already yielded behavioral and  
880 neuronal data without satiety (Pastor-Bernier et al., 2017; Pastor-Bernier et al., 2019). Neither  
881 animal had been used in any other study.

882  
883 **Ethical approval**

884 This research has been ethically reviewed, approved, regulated and supervised by the following  
885 institutions and individuals in the UK and at the University of Cambridge (UCam): the Minister of  
886 State at the UK Home Office, the Animals in Science Regulation Unit (ASRU) of the UK Home  
887 Office implementing the Animals (Scientific Procedures) Act 1986 with Amendment Regulations  
888 2012, the UK Animals in Science Committee (ASC), the local UK Home Office Inspector, the UK  
889 National Centre for Replacement, Refinement and Reduction of Animal Experiments (NC3Rs), the  
890 UCam Animal Welfare and Ethical Review Body (AWERB), the UCam Governance and Strategy  
891 Committee, the Home Office Establishment License Holder of the UCam Biomedical Service  
892 (UBS), the UBS Director for Governance and Welfare, the UBS Named Information and  
893 Compliance Support Officer, the UBS Named Veterinary Surgeon (NVS), and the UBS Named  
894 Animal Care and Welfare Officer (NACWO).

895  
896 **General behavior**

897 The animals were habituated during several months to sit in a primate chair (Crist Instruments) for a  
898 few hours each working day. They were trained in a specific, computer-controlled behavioral task  
899 in which they contacted visual stimuli on a horizontally mounted touch-sensitive computer monitor  
900 (Elo) located 30 cm in front of them. The animal's eye position in the horizontal and vertical plane  
901 were monitored with a non-invasive infrared oculometer (Iscan). Matlab software (Mathworks)  
902 running on a Microsoft Windows XP computer controlled the behavior and collected, analyzed and  
903 presented the data on-line. A solenoid valve (ASCO, SCB262C068) controlled by the same  
904 Windows computer served to deliver specific liquid amounts. A Microsoft SQL Server 2008  
905 Database served for Matlab off-line data analysis. Following task training for about 6 months,  
906 animals were surgically implanted with a recording chamber for electrophysiological recordings,  
907 which typically lasted for another 6-10 months.

908  
909 **Stimuli, task and rewards**

910 A computer touch monitor presented the subject with two visual stimuli (4° apart) representing two  
911 bundles, a Reference Bundle and a Variable Bundle (Figure 1A). Each bundle contained two

912 rewards (Component Reward A: violet rectangle, and component Reward B: green rectangle) with  
 913 independently set amounts indicated by the vertical bar position within each rectangle (higher was  
 914 more). The Reference Bundle contained two preset Reward amounts that were fixed for a given  
 915 block of trials. The Variable Bundle contained a specifically set amount of one Reward and an  
 916 experimentally varied amount of the other reward. The task sequence (Figure 1B) has been  
 917 described in detail (Pastor-Bernier et al., 2017; Pastor-Bernier et al., 2019) and are summarized as  
 918 follows. Reward A in all bundles was blackcurrant juice, or blackcurrant juice with added  
 919 monosodium glutamate (MSG), Reward B was grape juice, strawberry juice, mango juice, water,  
 920 apple juice, peach juice, or grape juice with added inosine monophosphate (IMG).

921 Each trial began when the animal contacted a centrally located touch sensitive key for 1.0 s  
 922 after a pseudorandom inter-trial interval of  $1.6 \pm 0.25$  s. Then two bundles appeared and remained  
 923 on the screen for 2.0 s, after which two blue spots appeared as GO stimulus underneath the bundles,  
 924 upon which the animal released the touch key and touched the blue spot of its choice within 2.0 s.  
 925 After a hold time of 1.0 s, the chosen blue spot turned green and the unchosen blue spot  
 926 disappeared. Simultaneously a white frame around the chosen bundle appeared providing feedback  
 927 for successful choice. The computer-controlled liquid solenoid valve delivered liquid A at 1.0 s  
 928 after the choice, followed 0.5 s later by liquid B (except when using peach juice as Reward B; here  
 929 the sequence was reversed: liquid B was delivered first, then 0.5 s later liquid A, blackcurrant  
 930 juice).

931

### 932 **Estimation of behavioral ICs**

933 The behavioral method used to obtain an IP from stochastic choice has been presented in full detail  
 934 (Pastor-Bernier et al., 2017; Pastor-Bernier et al., 2019). With two bundle options, the animal chose  
 935 between the pre-set Reference Bundle (left in Figure 1A) and the Variable Bundle (right) in  
 936 repeated trials. Thus, the constant Reference Bundle provided a stable reference against the  
 937 changing bundle composition in the Variable Bundle. We set one reward in the Variable Bundle to  
 938 one unit ( $\geq 0.1$  ml) above the amount of the same reward in the Reference Bundle, while  
 939 pseudorandomly varying the amount of the other reward widely. The variation of the animal's  
 940 repeated choice with that single varying Reward allowed us to construct a full psychophysical  
 941 function and estimate the IP from a Weibull fit (point of subjective equivalence;  $P = 0.5$  choice of  
 942 each bundle).

943 As in our previous study (Pastor-Bernier et al. 2017), we used the Matlab function GLMFIT  
 944 for psychophysical fitting. This function returns a number called 'Deviance' between 0 to infinity  
 945 that can be used to compare fitting between Weibull and logit. The Deviance is the difference  
 946 between the log-likelihood of the fitted model and the maximum possible log-likelihood. Lower  
 947 values are better. The estimated Deviance for psychophysics for the first 5,000 trials and 2 monkeys  
 948 was 1.0415 for the Weibull model and 1.6009 for the logit model, suggesting that the Weibull fitted  
 949 better the data. Hence, we used Weibull fitting for all psychophysical fitting.

950 We obtained each IP from a total of 80 trials (2 left-right stimulus positions with 5 equally  
 951 spaced Reward amounts in 8 trials). To avoid known adaptations in OFC neurons (Tremblay and  
 952 Schultz, 1999; Padoa-Schioppa, 2009; Kobayashi et al., 2010; Rustichini et al., 2017), we always  
 953 tested the full reward range of the experiment.

954 To obtain an IC, we fit a series of IPs with a hyperbolic function  $d$  using weighted least mean  
 955 squares:

956

$$957 \quad d = ay + bx + cxy \quad (\text{Eq. 1})$$

958

959 with  $y$  and  $x$  as milliliter amount of Reward A (plotted at  $y$ -axis on 2D graph, Figure 1C and 1E)  
 960 and Reward B (plotted at  $x$ -axis),  $a$  and  $b$  as weights of the influence of the Reward amounts plotted  
 961 on the  $y$ - and  $x$ -axes, respectively, and  $c$  as curvature. A potent reward that contributes strongly to  
 962 the choice of the bundle would have a large weight (high coefficient  $a$  or  $b$ ), whereas a less potent  
 963 reward would have lower weight coefficients. Thus, with the potent (more weight) reward plotted

964 on the x-axis, and the less potent (less weight) reward plotted on the y-axis, choice indifference  
 965 between them (IC) would occur with smaller milliliter amounts on the x-axis compared to the y-  
 966 axis. Hence, the IC slope would be steeper than the diagonal line (see Figure 1C, D). By resolving  
 967 Eq. 1 as  $y = -(b / a) * x$ , the IC slope would be the ratio of the coefficients that reflect the weights of  
 968 the rewards:  $-b / a$ . With a higher potency of Reward B (x-axis) compared to Reward B (y-axis), the  
 969 rectified IC slope would be larger than 1. Relatively stronger satiety for Reward B (x-axis)  
 970 compared to Reward A (y-axis) would reduce the weight of Reward B, reduce the absolute value of  
 971 the ratio  $-b / a$ , and flatten the IC slope. Thus, the IC slope  $-b / a$  describes the relative impact of the  
 972 two bundle rewards (reflecting the value ratio between the two rewards), whereas the weights (a and  
 973 b) describe the influence of the Reward amounts.

974 The hyperbolic function can be re-written in an equivalent form to the regression with  
 975 interaction used for analysing neuronal responses (see Eq. 3 below):

$$976 \quad y = \beta_0 + \beta_1 A + \beta_2 B + \beta_3 AB + \varepsilon \quad (\text{Eq. 1a})$$

977 with A and B as milliliter amount of Reward A (plotted at y-axis) and Reward B (x-axis),  
 978 respectively,  $\beta_0$  as offset coefficient,  $\beta_1$  and  $\beta_2$  as behavioral regression coefficients, and  $\varepsilon$  as  
 979 compound of errors  $\text{err}_0, \text{err}_1, \text{err}_2, \text{err}_3$  for offset and regressors 1-3.

982

### 983 **Definition and criteria for pre-sated and sated states**

984 With on-going reward consumption, the changes of psychophysical choice functions exceeding the  
 985 confidence intervals (CI) of initial tests suggested a changed value relationship between the two  
 986 bundle rewards suggestive of relative, reward-specific satiety (see Figures 1D, S1A, S1E). More  
 987 specifically, the gradual effect of satiety on choice preference was identified by tracking the IPs as  
 988 consumption advanced across blocks of 80 trials. Importantly, these changes occurred fast enough  
 989 to be studied during the recording durations of single neurons, thus allowing us to compare  
 990 responses between non-sated and sated states in the same neuron. The Weibull-fitted IPs were  
 991 obtained psychophysically for fixed and equally spaced amounts of Reward B. Changes in relative  
 992 value of the two bundle rewards were assessed with interleaved anchor trials in choices between  
 993 bundles with only one non-zero reward: bundle (fixed non-zero blackcurrant juice; no Reward B)  
 994 vs. bundle (no blackcurrant juice; variable non-zero Reward B), using any Reward B (Figure S1B).  
 995 To aggregate IP data across sessions and compensate for across-session variability, we normalized  
 996 the reward value ratio to the first titration block in all sessions. We then compared the normalized  
 997 distributions of IPs within the CI of the first block with the distributions of IPs exceeding the CI of  
 998 the first block.

999

### 1000 **Control regressions for behavioral choice**

1001 To test whether the animal's choice reflected the amount of the bundle rewards during satiety,  
 1002 rather than other, unintended variables such as spatial bias, we used the logistic regression

1003

$$1004 \quad P(V) = \beta_0 + \beta_1 CT + \beta_2 RA + \beta_3 RB + \beta_4 VA + \beta_5 VB + \beta_6 CL + \beta_7 MA + \beta_8 MB + \varepsilon \quad (\text{Eq. 2})$$

1005

1006 with  $P(V)$  as probability of choice of Variable Bundle,  $\beta_0$  as offset coefficient,  $\beta_1 - \beta_7$  as  
 1007 correlation strength (regression slope) coefficients indicating the influence of the respective  
 1008 regressor, CT as trial number within block of consecutive trials, RA as amount of Reward A of  
 1009 Reference Bundle, RB as amount of Reward B of Reference Bundle, VA as amount of Reward A of  
 1010 Variable Bundle, VB as amount of Reward B of Variable Bundle, CL as choice of any bundle  
 1011 stimulus presented at the left, MA as consumed amount of Reward A, MB as consumed amount of  
 1012 Reward B, and  $\varepsilon$  as compound error for offset and all regressors. We used a binomial fit with logit  
 1013 link function to obtain standardized  $\beta$  coefficients. Choices over zero-reward bundles were excluded  
 1014 in the regression to avoid internal correlation between value and consumption.

1015

## 1016 **Licking**

1017 Licking was monitored with an infrared optosensor positioned below the juice spout (V6AP; STM  
1018 Sensors). Anticipatory licking durations were measured between the appearance of the bundle  
1019 stimuli and delivery of the first reward liquid (approximate duration 5 - 6 s) in bundles containing  
1020 only one non-zero component reward with advancing trials in satiety and within single working  
1021 sessions. Licking data were collected with four different bundles, namely (blackcurrant juice, grape  
1022 juice), (blackcurrant juice, water), (blackcurrant juice, strawberry juice) and (blackcurrant juice,  
1023 mango juice).

## 1025 **Surgical procedures and electrophysiology**

1026 As described before for the same animals (Pastor-Bernier et al., 2019), a head-restraining device  
1027 and a recording chamber (40 x 40 mm, Gray Matter) were implanted on the skull under full general  
1028 anesthesia and aseptic conditions. The stereotactic coordinates of the chamber enabled neuronal  
1029 recordings of the orbitofrontal cortex (OFC) (Paxinos et al., 2000). We located the OFC from bone  
1030 marks on coronal and sagittal radiographs taken with a guide cannula inserted at a known  
1031 coordinate in reference to the implanted chamber, using a medio-lateral vertical and a 20° degree  
1032 forward directed approach aiming for area 13. Monkey A provided data from the left hemisphere,  
1033 Monkey B from the right hemisphere, via a craniotomy in each animal ranging from Anterior 30 to  
1034 38, and Lateral 0 to 19. We conducted single-neuron electrophysiological recordings using both  
1035 custom made glass-coated tungsten electrodes (Merrill & Ainsworth, 1972), and commercial  
1036 electrodes (Alpha Omega, Israel) (impedance of about 1 MOhm at 1 kHz). Electrodes were inserted  
1037 into the cortex with a multi-electrode drive (NaN drive, Israel) with the same angled approach as  
1038 used for the radiography. Neuronal signals were collected at 20 kHz, amplified using conventional  
1039 differential amplifiers (CED 1902 Cambridge Electronics Design) and band-passed filtered (high:  
1040 300 Hz, low: 5 kHz). We used a Schmitt-trigger to digitize the analog neuronal signal online into a  
1041 computer-compatible TTL signal. However, we did not use the Schmitt-trigger to separate  
1042 simultaneous recordings from multiple neurons, in which case we searched for another recording  
1043 from only a single neuron, or we stored occasionally the data in analog form for off-line separation  
1044 by dedicated software (Plexon offline sorter). An infrared eye tracking system monitored eye  
1045 position (ETL200; ISCAN), with temperature check on an experimenter's hand at the approximate  
1046 position of the animal's head.

## 1048 **Definition for neurons following the revealed preference scheme**

1049 We analysed single-neuron activity during four task epochs vs. Pretrial control (1 s): visual Bundle  
1050 stimulus (2 s), Go signal (1 s), Choice (1 s) and Reward (2 s, starting with Reward A, followed 0.5 s  
1051 later by Reward B, thus covering both rewards). To establish neuronal relationships to these task  
1052 epochs, we compared the activity in each neuron during each task epoch separately against the  
1053 Pretrial control epoch using the paired Wilcoxon test ( $P < 0.01$ ). A neuron was considered task-  
1054 related if its activity in at least one of the four task epochs differed significantly from the activity  
1055 during the Pretrial control epoch.

1056 Responses of individual neurons should follow the scheme of two-dimensional ICs that  
1057 characterizes revealed behavioral preferences for two-dimensional bundles. Specifically, the  
1058 responses should comply with three characteristics defined previously (Pastor-Bernier et al., 2019).

1059 (Characteristic 1) Neuronal responses should change monotonically with increasing  
1060 behavioral preference *across behavioral ICs*, irrespective to bundle composition. Such monotonic  
1061 neuronal response changes should reflect increasing amounts of one or both bundle rewards,  
1062 assuming a positive monotonic subjective value function on Reward amount.

1063 (Characteristic 2) Neuronal responses should vary insignificantly for all equally preferred  
1064 bundles positioned *along a same behavioral IC*, despite different physical bundle composition.

1065 (Characteristic 3) Neuronal responses should follow the IC slope and the non-linear curvature  
1066 of behavioral ICs. The IC slope reflects the value relationship between the two bundle rewards,

1067 indicating the revealed preference relation between the two rewards of a bundle, and thus the value  
1068 of one reward relative to a common reference reward.

1069 We used a combination of three statistical tests to assess these characteristics.

1070 Characteristic 1: To capture the change *across ICs* in the most conservative, assumption-free  
1071 manner possible, we used a simple linear regression on each Wilcoxon-identified task-related  
1072 response:

$$1073 \quad y = \beta_0 + \beta_1 A + \beta_2 B + \beta_3 AB + \varepsilon \quad (\text{Eq. 3})$$

1074 with  $y$  as neuronal response in any of the four task epochs, measured as impulses/s and z-scored  
1075 normalized to the Pretrial control epoch of 1.0 s (z-scoring of neuronal responses applied to all  
1076 regressions listed below),  $A$  and  $B$  as milliliter amount of Reward A (plotted at y-axis) and Reward  
1077 B (x-axis), respectively,  $\beta_0$  as offset coefficient,  $\beta_1$  and  $\beta_2$  as neuronal regression coefficients, and  
1078  $\varepsilon$  as compound error for offset and all regressors.

1081 The coefficients  $\beta_1$  and  $\beta_2$  needed to be either both positive (indicating positive neuronal  
1082 relationship, higher neuronal activity reflecting more reward quantity) or both negative (inverse  
1083 neuronal relationship) to reflect the additive nature of the individual bundle components giving rise  
1084 to revealed preference ( $P < 0.05$ , unless otherwise stated; t-test).

1085 This linear regression assessed the degree of linear monotonicity of neuronal response change  
1086 across ICs ( $P < 0.05$  for  $\beta$  coefficients; t-test). Further, all significant positive or negative response  
1087 changes identified by Eq. 3 needed to be also significant in a Spearman rank-correlation test that  
1088 assessed ordinal monotonicity of response change across ICs without assuming linearity and  
1089 numeric scale ( $P < 0.05$ ).

1090 Characteristics 1 and 2: To assess the two-dimensional *across/along IC* scheme in a direct and  
1091 intuitive way, and without assuming monotonicity, linearity and numeric scale, we used a two-  
1092 factor Anova on each Wilcoxon-identified task-related response that was significant for both  
1093 regressors in Eq. 3; the factors were *across-IC* (ascending rank order of behavioral ICs) and *along-*  
1094 *IC* (same rank order of behavioral IC). To be a candidate for following the IC scheme of Revealed  
1095 Preference Theory, changes across-ICs should be significant ( $P < 0.05$ ), changes within-IC should  
1096 be insignificant, and their interaction should be insignificant.

1097 Characteristic 3: Whereas the regression defined by Eq. 3 estimated neuronal responses across  
1098 ICs, a full estimation of neuronal ICs for comparison with behavioral ICs would require inclusion of  
1099 the IC slope and curvature, both of which depended on both rewards. By simplifying Eq. 3 by  
1100 setting to zero both the  $\beta_3$  coefficient and the constant neuronal response along the IC, the neuronal  
1101 IC slope would be the ratio of coefficients ( $-\beta_2 / \beta_1$ ). Note the different meanings of the slope term:  
1102 the neuronal IC slope ( $-\beta_2 / \beta_1$ ) describes the relative coding strength of the two bundle rewards  
1103 (reflecting the neuronal ratio of the two rewards), whereas each neuronal regression slope alone ( $\beta$ )  
1104 describes the coding strength of neuronal response (correlation with the specific regressor). The  
1105 neuronal IC curvature was estimated from the  $\beta_3$  coefficient of the interaction term AB (all  $\beta$ 's  $P <$   
1106  $0.05$ ; t-test).

1107  
1108 **Neuronal chosen value coding.** As stated before (Pastor-Bernier et al. 2019), chosen value (CV)  
1109 was defined as the value of a choice option the animal considered, would obtain or had obtained by  
1110 its choice. As each option consisted of two components, we used a linear combination of the  
1111 quantity of the two component rewards A (blackcurrant juice) and B (any of the other five rewards):

$$1112 \quad CV = A + k_1 B \quad (\text{Eq. 4})$$

1113 Weighting parameter  $k_1$  served to adjust for differences in subjective value between rewards A and  
1114 B, such that the quantity of Reward B entered the regression on a common-currency scale defined  
1115 by Reward A. We established parameter  $k_1$  during neuronal recording sessions from behavioral  
1116 choice IPs using quantitative psychophysics in anchor trials (80 trials per test, see above Trial types

1117 for neuronal tests), rather than reading it from fitted ICs. Thus,  $k_1$  equals the ratio of coefficients  $\beta_2$   
 1118 /  $\beta_1$  of Eq. 3.

1119 We established a common-currency scale in ml for all tested rewards by defining blackcurrant  
 1120 juice or blackcurrant-MSG (Reward A) as reference (numeraire); the subjective value of any reward  
 1121 is expressed as real-number multiple  $k_1$  of the quantity of the numeraire at choice indifference.  
 1122 Specifically, the animal chose between the Variable Bundle that contained a psychophysically  
 1123 varied quantity of blackcurrant juice (the other bundle reward being set to 0 ml) and the Reference  
 1124 Bundle that contained a fixed quantity of the other reward (blackcurrant juice being set to 0 ml). At  
 1125 choice indifference, the quantity of blackcurrant juice (Reward A) in the Variable Bundle defined  
 1126 the common-currency value of the other reward, from which we calculated parameter  $k_1$  as  $A / B$ . A  
 1127  $k_1$  of  $< 1$  indicated that more quantity was required for choice indifference against blackcurrant  
 1128 juice; thus,  $k_1 < 1$  suggested that the tested reward had lower subjective value than blackcurrant  
 1129 juice. By contrast,  $k_1 > 1$  suggested higher subjective value, as less quantity was required for choice  
 1130 indifference.

1131 We assessed the coding of chosen value and unchosen value in all neurons that followed the  
 1132 revealed preference scheme, using the following regression:

$$1133 \quad y = \beta_0 + \beta_1 CV + \beta_2 UCV + \varepsilon \quad (\text{Eq. 5})$$

1134 with UCV as value of the unchosen option that was not further considered here, and  $\varepsilon$  as compound  
 1135 error for offset and all regressors.

1136

1137 **Vector plots of OFC reward sensitivity.** The purpose of this analysis was to provide  
 1138 quantitative and graphic information about satiety-induced behavioral and neuronal changes that  
 1139 would allow comparison with previous OFC studies that had not used two-component choice  
 1140 options with individually varying reward amounts and therefore did not establish ICs (Padoa-  
 1141 Schioppa & Assad 2006). This simplified analysis addressed monotonic response increase or  
 1142 decrease with increasing amounts of bundle rewards across ICs (characteristic 1 above), but did not  
 1143 address other IC characteristics such as trade-off, slope and curvature (characteristics 2 and 3) that  
 1144 had not been investigated previously. We established 2D plots whose dots indicated the relative  
 1145 contribution of each of the two bundle rewards to the neuronal response. We then compared vectors  
 1146 of behavioral choices with vectors of averaged neuronal population responses before and during  
 1147 satiety.

1148 For behavioral choices, we plotted vectors (with 95% CIs) from averaged dot positions  
 1149 defined by reward amount (distance from center:  $\sqrt{\beta_1^2 + \beta_2^2}$ ) and relative weight (elevation  
 1150 angle:  $\arctan(\beta_1 / \beta_2)$ ); coefficient  $\beta_1$  refers to Reward A (blackcurrant, y-axis), coefficient  $\beta_2$   
 1151 refers to any of the other rewards (x-axis) (Eq. 1a). The angle of the vector reflects the relative  
 1152 contribution the two bundle rewards to the choice, as estimated by the a and b coefficients (Eq. 1).  
 1153 A deviation of the alignment angle from the diagonal line indicates an unequal contribution weight  
 1154 to bundle choice, and thus a non-1:1 reward ratio.

1155 For neuronal responses, each dot on the 2D plot was defined by the two  $\beta$  regression  
 1156 coefficients for neuronal responses (Eq. 3;  $P < 0.01$ , t-test) for each of the two rewards in any of the  
 1157 four task epochs. The distance from center indicates the z-scored response magnitude ( $\sqrt{\beta_1^2 +$   
 1158  $\beta_2^2}$ ), coding sign (positive or negative), and relative weight (elevation angle;  $\arctan(\beta_1 / \beta_2)$ )  
 1159 of the two  $\beta$  coefficients. Coefficient  $\beta_1$  refers to Reward A (blackcurrant, y-axis), coefficient  $\beta_2$   
 1160 refers to any of the other rewards (x-axis). Responses with negative (inverse) coding were rectified.  
 1161 Further IC characteristics such as systematic trade-off across multiple IPs and IC curvature played  
 1162 no role in these graphs. The alignment of the dots along the diagonal axis shows the relative coding  
 1163 strength for the two bundle rewards, as estimated by the  $\beta$  regression coefficients; a deviation from  
 1164 the diagonal line indicates an unequal influence of the two bundle rewards on the neuronal  
 1165 responses, reflecting a neuronal correlate of reward ratio.

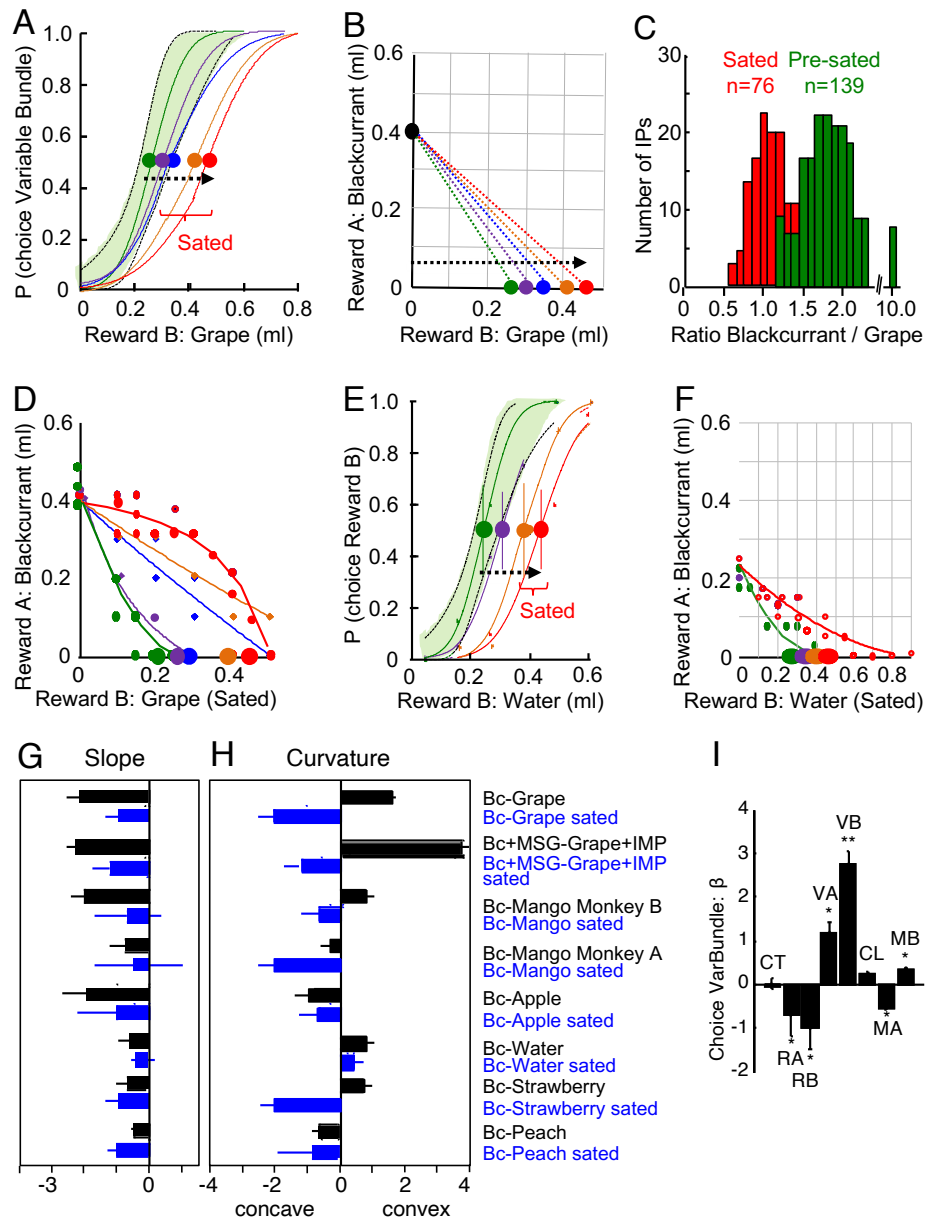
1166

1167 **Neuronal decoders**

1168 We used linear support vector machine (SVM) algorithms to decode neuronal activity according to  
1169 bundles presented at different behavioral ICs during choice over zero-reward bundle (bundle  
1170 distinction) and, separately, according to the behavioral choice between two non-zero bundles  
1171 located on different ICs (choice prediction). As in our main study on revealed preferences (Pastor-  
1172 Bernier et al., 2019), we implemented both decoders as custom-written software in Matlab R2015b  
1173 (Mathworks). The SVM decoder with linear kernel was accomplished with `svmtrain` and  
1174 `svmclassify` procedures (our previous work had shown that use of nonlinear SVM kernels does not  
1175 improve decoding Tsutsui et al., 2016). The SVM decoder was trained to find the optimal linear  
1176 hyperplane for the best separation between two neuronal populations relative to lower vs. higher  
1177 ICs.

1178 All analyses employed single-neuron data, consisting of single-trial impulse counts that had  
1179 been z-normalised to the activity during the Pretrial epoch in all trials recorded with the neuron  
1180 under study. The analysis included activity from all neurons whose responses followed the IC  
1181 scheme of revealed preferences during any of the four task epochs, as identified by our three-test  
1182 statistics, except where noted. The neurons were recorded one at a time; therefore, the analysis  
1183 concerned aggregated pseudo-populations of neuronal responses.

1184 The decoding analysis used 10 trials per neuron for each of two ICs (total of 20 trials).  
1185 Extensive analysis suggested that higher inclusion of 15-20 trials per group did not provide  
1186 significantly better decoding rates (while reducing the number of included neurons). For neurons  
1187 that had been recorded with  $> 10$  trials per IC, we selected randomly 10 trials from each neuron for  
1188 each of the two ICs. We used a leave-one-out cross-validation method in which we removed one of  
1189 the 20 trials and trained the SVM decoder on the remaining 19 trials. We then used the SVM  
1190 decoder to assess whether it accurately detected the IC of the left-out trial. We repeated this  
1191 procedure 20 times, every time leaving out another one of the 20 trials. These 20 repetitions resulted  
1192 in a percentage of accurate decoding (% out of  $n = 20$ ). The final percentage estimate of accurate  
1193 decoding resulted from averaging the results from 150 iterations of this 20-trial random selection  
1194 procedure. To distinguish from chance decoding, we randomly shuffled the assignment of neuronal  
1195 responses to the tested ICs, which should result in chance decoding (accuracy of 50% correct). A  
1196 significant decoding with the real, non-shuffled data would be expressed as statistically significant  
1197 difference against the shuffled data ( $P < 0.01$ ; Wilcoxon rank-sum test).  
1198

1200  
1201

1202

**Figure S1. Additional behavioral measures**

1203

1204

1205

1206

1207

1208

1209

1210

1211

1212

1213

1214

1215

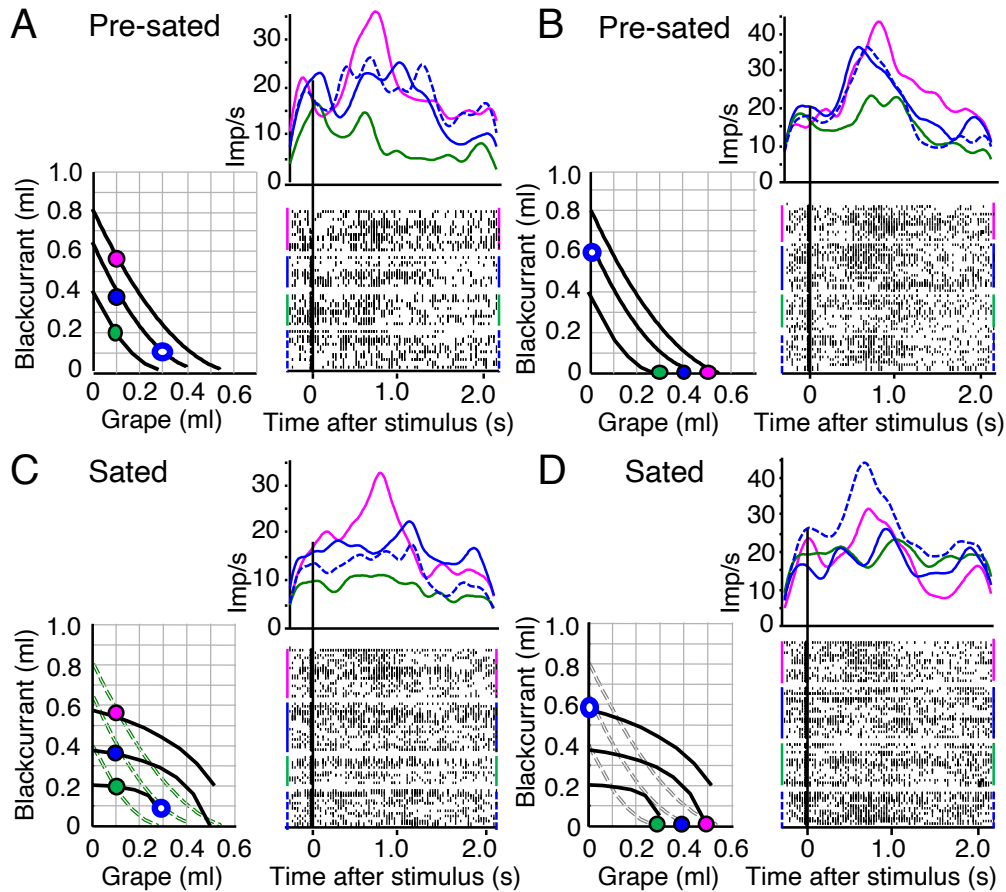
1216

1217

(A) Psychophysical assessment of choice between single-reward bundles with grape juice variation (constant Reference Bundle: 0.6 ml blackcurrant juice, 0.0 ml grape juice; Variable bundle: 0.0 ml blackcurrant juice, varying grape juice). Green and violet curves inside green  $\pm 95\%$  confidence intervals: initial choices; blue, orange and red curves: on-going consumption. The decrease in ratio blackcurrant/grape juice amounts at IP was significant between the confidence interval of the first IP and all IPs exceeding it (ratios of  $1.9857 \pm 0.0173$ ,  $N = 139$ , green, vs.  $1.0077 \pm 0.02$ , orange and red; mean  $\pm$  standard error of the mean, SEM; individual trial blocks:  $p = 9.6943 \times 10^{-7}$ , Kolmogorov-Smirnov test;  $p = 2.336 \times 10^{-32}$ , Wilcoxon rank-sum test;  $p = 3.1712 \times 10^{-46}$ , t-test; Monkey A). Each curve and indifference point (IP) were estimated from 80 trials in a single block (Weibull fits).

(B) Gradually developing relative satiety for grape juice indicated by increasing choice indifference points (IP; same bundles and animal as in A): with on-going consumption of both juices, the animal gave up progressively more grape juice for obtaining the same 0.4 ml of blackcurrant juice (from green to red). The ratio blackcurrant/grape juice amounts at IP decreased from approximately 2:1 (0.4 ml of blackcurrant juice for 0.25 ml of grape juice, black vs. green dots) to about 1:1 (0.4 ml

1218 blackcurrant for 0.45 ml grape juice, black vs. red), suggesting subjective value loss of grape juice  
1219 relative to blackcurrant juice.  
1220 (C) Significant decrease of ratio blackcurrant/grape juice amounts at IP with on-going consumption  
1221 (same bundles as in A; Wilcoxon test). N = 139 and 76 IPs estimated in 43 trial blocks (Monkey A).  
1222 (D) Gradual changes with grape juice variation in slope and curvature of choice indifference curves  
1223 (IC) between pre-satiety (green, violet) and during increasing satiety (blue, orange, red) (single  
1224 session; 2,960 trials; 80 trials/IP; Monkey A).  
1225 (E), (F) Psychophysical tests and consumption-dependent change of ICs in Monkey B during choice  
1226 between single-component bundles (constant Reference Bundle: 0.25 ml blackcurrant juice, 0.0 ml  
1227 water; Variable bundle: 0.0 ml blackcurrant juice, varying water). With on-going consumption of  
1228 both liquids, the animal gave up progressively more water for obtaining the same 0.25 ml of  
1229 blackcurrant juice (from green to red), suggesting subjective value loss of water relative to  
1230 blackcurrant juice. Same conventions as in A and D (2,400 trials; 80 trials/IP), Monkey B.  
1231 (G), (H) Significant IC slope and curvature changes from pre-sated to sated states with on-going  
1232 consumption with individual bundles (Bc, blackcurrant juice; MSG, monosodium glutamate; IMP,  
1233 inosine monophosphate;  $p = 0.0156$  and  $p = 0.0313$ , respectively; Wilcoxon test). The slope  
1234 parameter reflects the amount ratio blackcurrant/other liquids at IP.  
1235 (I) Value control by logistic regression for choice of Variable Bundle over non-zero Reference  
1236 Bundle during satiety (Eq. 2). According to significance of  $\beta$  regression coefficients, choice of the  
1237 Variable Bundle (Choice VarBundle) correlated significantly with amount of rewards A and B in  
1238 the Variable Bundle (VA, VB) and the Reference Bundle (RA, RB) and the consumed amount of  
1239 bundle rewards A (blackcurrant; MA) and B (various other liquids; MA). Choice varied  
1240 insignificantly with consecutive trial number within blocks (CT) and left-right choice (CL). N =  
1241 7,243 trials pooled from several sessions; \*  $P < 0.05$ ; \*\*  $P < 0.01$ ; t-test on  $\beta$ s.  
1242



1244

1245

1246

1247

1248

1249

1250

1251

1252

1253

1254

1255

1256

1257

1258

1259

1260

1261

1262

1263

1264

1265

1266

1267

1268

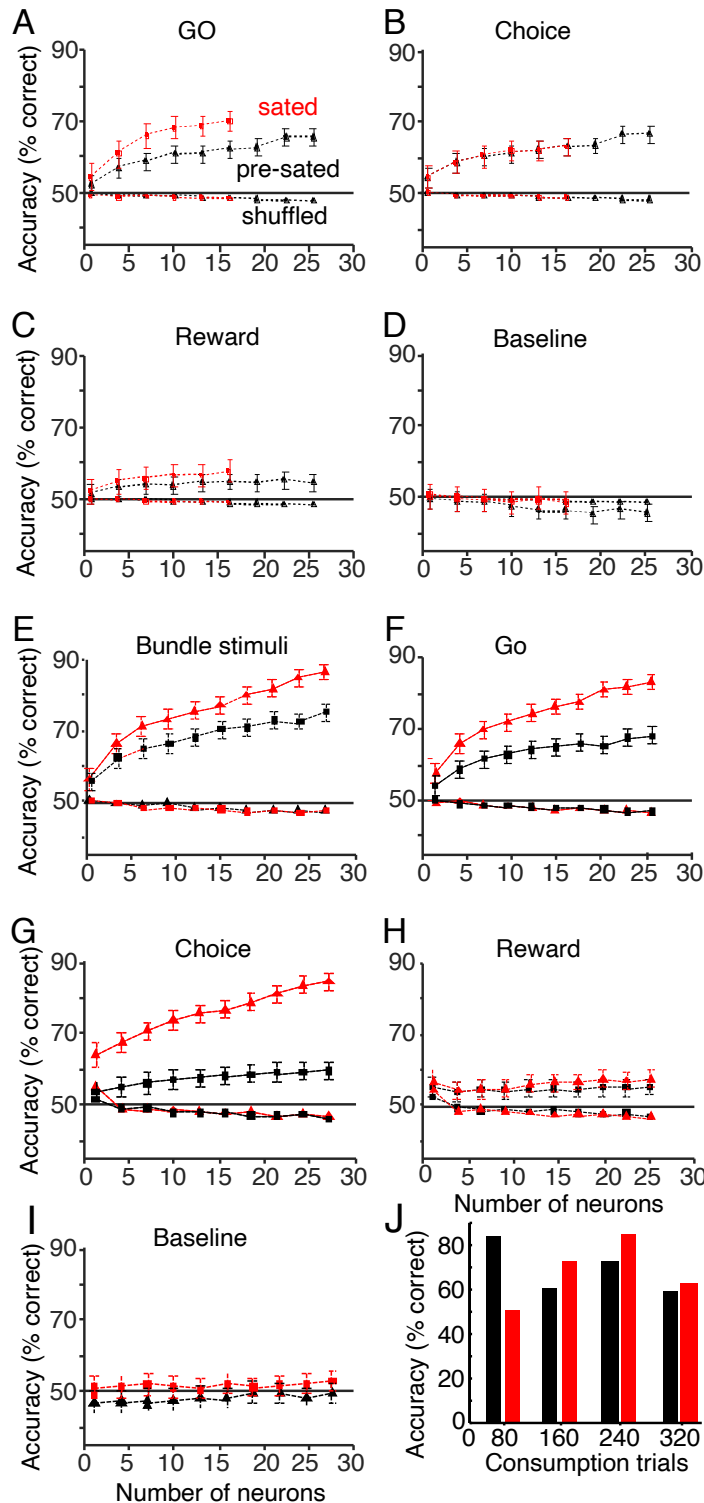
### Figure S2. Satiety-related neuronal response change during choice between two non-zero bundles

(A) Significant monotonic neuronal response increase with value of chosen bundle across indifference curves (IC) before satiety (from green via blue to red) ( $P = 0.0055$ ,  $F = 10.49$ , 17 trials; 1-way Anova). The animal chose between the Reference Bundle (hollow blue dot) and one of the Variable Bundles (solid colored dots). The responses to the two blue bundles on the same IC (indicating equal preference) varied insignificantly despite different juice composition ( $P = 0.5488$ ,  $F = 0.38$ , 18 trials). Response to Reference Bundle (hollow blue dot) is indicated by dotted line.

(B) As (A) but for grape juice variation. Responses varied significantly across ICs with grape juice ( $P = 0.0046$ ,  $F = 9.7$ , 27 trials). The responses to the two blue bundles on the same IC differed insignificantly ( $P = 0.2622$ ,  $F = 1.31$ , 29 trials). Same color labels as in (A).

(C) Despite IC change indicating satiety, the neuronal response increase across ICs remained significant ( $P = 0.0014$ ,  $F = 10.87$ , 17 trials). However, the two unchanged blue bundles were now on different ICs, and their responses varied significantly ( $P = 0.0028$ ,  $F = 5.46$ , 40 trials).

(D) With slope and curvature change indicating satiety, the three bundles with grape juice variation were now located within only two ICs. Although the neuronal response increase across ICs remained significant ( $P = 0.0144$ ,  $F = 6.02$ , 35 trials), the peak response was reduced by 25% (from 40 to 30 imp/s, red) and the three responses were closer to each other. Further, the two unchanged blue bundles were now on different ICs, and their responses now differed significantly ( $P = 0.0201$ ,  $F = 9.27$ , 52 trials). Thus, the changes of neuronal responses were consistent with the IC change indicating satiety.



1270

1271

1272 **Figure S3. Satiety-induced changes in bundle classification during different task epochs**  
 1273 (A) - (D) Choice over zero-bundle. Baseline refers to 1 s Pretrial control epoch before Bundle  
 1274 stimuli. For details, see Figure 6.

1275 (E) - (I) As (A-D) but for choice prediction by neuronal responses during choice over non-zero  
 1276 bundle.

1277 (J) Classification accuracy of neuronal responses across on-going liquid consumption. Same data  
 1278 selection as for (A-D) and collapsed across all task epochs. Black: before satiety, red: during satiety.

1279